# Comparison of Lift Path Planning Algorithms for

# Mobile Crane Operations in Heavy Industrial Projects

**Serim Park**

A Thesis

in

The Department

of

Building, Civil and Environmental Engineering

Presented in Partial Fulfillment of the Requirements

for the Degree of Master of Applied Science (Civil Engineering) at

Concordia University

Montreal, Quebec, Canada

January 2020

# CONCORDIA UNIVERSITY

## School of Graduate Studies

This is to certify that the thesis prepared

By:               Serim Park

Entitled:         Comparison of Lift Planning Algorithms for Mobile Crane Operations in
                  Heavy Industrial Project

and submitted in partial fulfillment of the requirements for the degree of

**Master of Applied Science (Civil Engineering)**

complies with the regulations of the University and meets the accepted standards with respect to originality and quality.

Signed by the final Examining Committee:

_____Dr. F. Nasiri_____ Chair

_____Dr. A. Hammad_____ Examiner

_____Dr. M. Nik-Bakht_____ Examiner

_____Dr. S. H. Han_____ Supervisor

Approved by      _____Dr. A. Bagchi_____
                 Chair of Department or Graduate Program Director

                 _____Dr. A. Asif_____
                 Dean of Faculty

         Date    _____

# ABSTRACT

## Comparison of Lift Planning Algorithms for Mobile Crane Operations in Heavy Industrial Project

Serim Park

Heavy industrial projects, especially oil refineries, are constructed by modules prefabricated in factories, transported to sites and installed by mobile cranes. Due to a large number of lifts on the congested and dynamic site layouts in heavy industrial projects, the lift path planning has been attention for not only safe and efficient mobile crane operation but also better project productivity and safety. Although the path planning algorithms have been introduced over the years, they have not been used actively in practice since the comparison of these algorithms has not been examined yet based on the realistic mobility of mobile cranes and real site environment. Therefore, this thesis compares the path planning algorithms including A* search, rapidly-exploring random tree (RRT), genetic algorithms (GA) and 3D visualization-based mathematical algorithm (3DVMA) under the same site environment in order to find a competent method using measurement metrics considering collision-free and optimal lift paths with the lower crane operation cost and less computation time. The proposed comparison is implemented in a case study that includes a series of modules lifted by a mobile crane on various site conditions. This comparison shows the advantages and disadvantages of each algorithm for the crane path planning in heavy industrial projects and suggests the direction of further research in this field.

# ACKNOWLEDGEMENTS

# Table of Contents

# LIST OF FIGURES

# LIST OF TABLES

# Chapter 1:  INTRODUCTION

## 1.1  Introduction

Modular construction, which is also known as off-site construction, delivers the pre-assembled modules to sites; it is increasingly recognized as a cost-effective method that reduces on-site labor usage, material waste, and construction time for project safety and productivity improvement. Because of these benefits, a modular approach has been widely adopted particularly in apartment buildings and heavy industrial projects [1, 2]. Heavy industrial projects have several characteristics: *(i)* an numerous lifting operations on large scale sites; *(ii)* dynamic site layouts that are changed in accordance with the lifting sequences; and (*iii*) a large  mobile crane configuration mounted a superlift (counterweight) to allow the crane lift heavy objects.. Mobile cranes are commonly used to install the modules on their positions at project sites due to its high capacity, thus efficient and safe utilization of the mobile crane is a key for successful completion of the modular projects. In other words, insufficient planning and analysis of crane utilizations can cause not only productivity reduction but also result in accidents with high fatality rates. According to a report on the causes of death in crane-related accidents [3], at least 71% of all crane-related fatal accidents are involved with mobile cranes, which are caused by crane collapses (39%), overhead power line contacts (14%), struck by crane load (14%), struck by other crane parts (11%), and other causes such as highway incidents, falls, and caught in/between (23%). To reduce these crane accidents, a considerable number of algorithms and methodologies have been introduced to generate collision-free crane lift paths in the construction domain using computer-aided computation and simulation technologies that satisfy the three main factors for the successful lift path planning: efficiency, solution quality, and success rate [4].

The conventional manual lift analysis by lift engineers is not suitable in heavy industrial projects including a number of modules which requires considerations of all lifting alternatives rapidly without errors [5]. In early adaptation phase of the lift analysis, an interactive computer-aided planning environment (COPE) was proposed for critical and heavy lifts [6, 7]. According to advanced technologies, automatic lift path planning systems have been introduced by using mathematical methods and optimization algorithms; yet, these endeavors do not sufficiently address the practical requirements which considers the dynamic and congested site layouts, least crane motions, and the complexity of crane lift constraints [2, 8, 9]. For example, the lift path planning is developed using hill climbing, A* algorithm, and genetic algorithm (GA) based on the configuration space (C-space), that can represent high degrees of freedom (DOF) environment effectively for the single crane and cooperative crane operations [10–12]. Cai et al. [4] have proposed parallel GA applying hybrid configuration concepts to handle complex site conditions based on considering energy cost, human cost, and workability of operator while overcoming collisions and crane constraints. Additionally, the research by Chang et al. [13] has used a probabilistic road-map (PRM) method for the crane erection planning as near real-time solutions. Rapidly exploring Random Trees (RRT), as one of the popular randomized path planning algorithms in robotics, has been introduced by several researchers for lifting path planning [14–16]. Also, the multiagent-based approach [17] has been developed to not only avoid collision but also re-plan the paths in real-time lifting process.

Although previous attempts have introduced numerous algorithms and methodologies to plan optimal lift paths for mobile crane operations, these efforts have not fully been adapted yet in the heavy industrial sector due to the lack of the following requirements: *(i)* design times of collision-free lift paths on practical site environment which is reflected by the features of heavy

industrial projects; *(ii)* applicability of natural and realistic mobility of mobile cranes (e.g., step resolution and safety factor considering for estimating the cycle times of crane operations) based on practical crane lift rules depending on the company regulation; and *(iii)* advantages and disadvantages of algorithms which can be used to select an optimal algorithm in accordance with the features of heavy construction projects (e.g., congested and dynamic site layout changes). In terms of the step resolution for luffing, swing, and hoisting motions of mobile cranes during running algorithms, previous research has adopted (10, 5, 2) per step which can lead to not only prevent the crane lift paths reach to the destination exactly but also neglect possible collisions. In this respect, this thesis set (1, 1, 1) per step reflecting the realistic motions of mobile cranes.

To address this information, this thesis implements the comprehensive comparison of lift paths using existing algorithms, which are A* search, RRT, GA, and 3D visualization-based mathematical algorithm (3DVMA), based on measurement metrics. The results of this comparison can not only identify the well-performed crane lift path algorithm for heavy industrial projects but also provide directions of future research to develop a new algorithm in crane lift path planning if the existing algorithms do not satisfy the requirements described above. At this junction, it should be noted that this thesis selects algorithms used to design mobile crane lift paths in the previous researches based on the following reasons: *(i)* algorithms are selected among the previously implemented algorithms for optimal mobile crane lift paths based on the most common adoption and different searching methods;; *(ii)* A* tends to find the optimal path using an admissible heuristic function with the high accuracy; *(iii)* RRT is a randomized algorithm by building a space-filling tree biased toward the unsearched area to solve problems with high DOFs on sites which have numerous obstacles; *(iv)* GA is an evolutionary algorithm inspired by the natural selection used to design optimal crane lifts; and *(v)* 3DVMA as a recent work is the combination of

3

mathematical methods and 3D visualization to plan crane lift paths for heavy industrial projects. The comparison of these algorithms is implemented in a real heavy industrial project.

## 1.2   Research Objectives

The research is proposed to:

1) Appling path planning algorithms into the crane lift path problems in heavy industrial projects with the consideration of the practical site environment and realistic crane mobility.

2) Comparing the quality of the results based on the multi-measurement matrix and site constraints.

3) Providing a guidance to select the algorithm based on the characteristics of the heavy industrial projects.

4) Introducing the direction of lift path planning algorithm for mobile crane that integrates the advantages of compared algorithms.

## 1.3  Structure of Thesis

The overall structure of the study takes the form of five chapters, including this introductory Chapter 1. Chapter 2 begins by laying out the literature review that introduces the recent and significant topics regarding simulation and automation in construction, path planning algorithms, and their implementation in construction industry and comparison. Chapter 3 is concerned with the methodology used for this study. It first explains the structural basis that applied in common to three algorithms (A*, RRT, and GA) in terms of problem formulation, crane constraint, and collision detection. Second, the development process of each algorithm is proposed. Chapter 4 presents the detail of case project and the results of four cases by applying the methodology from Chapter 3. Visualized path images and the comparison results are provided. Finally, Chapter 5 includes a brief summary and a discussion of the implication of the findings to future research into this area.

# Chapter 2: LITERATURE REVIEW

## 2.1 Introduction

To provide a constructive analysis, this section reviews the previous researches regarding simulation/automation in the construction industry, path planning algorithms, and comparison of path planning algorithms for the crane operation. This ensures that this research avoids duplicated works and identifies inconsistencies and gaps to discover the safe and efficient algorithm by comparing widely used path planning algorithms for the crane lift planning.

## 2.2 Simulation and Automation in Construction Operation

### 2.2.1 General

Computer-aided system has been implemented widely in construction industry to achieve improved efficiency and safety. For the purpose of generic maintenance, several studies regarding site layout and construction planning have been carried out. For instance, Chen et al. [18] developed an automated site layout system called ArcSite, which combines a geographic information system (GIS) with data management systems (DBMSs) to generate the design of temporary facilities (TF) automatically for the optimal site. The proposed system uses the elimination technique to find the best location for each facility. A study by Mawdesley et al. [19] integrated genetic algorithm to solve site layout problem by formulating the relationship between temporary facilities, access, and connection to generate the low site cost layout. Simulation in two cases proved the feasibility of the system while arising the necessity of integrating time parameter and the level of detail. Later, Sanad et al. [20] suggested optimization model for the site layout using genetic algorithm that considered the aspect of safety and environment. Furthermore, with the consideration of site space change over time, dynamic site planning is required. In this aspect,

Xu et al. [21] proposed a multi-objective decision making system with the fuzzy random uncertainty to provide more realistic solution that minimize the total cost and maximize the distance between the facilities that have potential risk. For tower cranes, a mixed-integer linear program (MILP) was introduced to suggest an efficient layout of a single tower crane in the confined site. The authors concluded that MILP optimized the site layout problem resulting in 7 % less cost of the total material transportation than GA algorithm with more flexibility to add potential constraints [22].

As narrow down to the crane related topic in the crane, crane type selection and location become initial subtasks in site planning. Hanna el al. [23] developed a fuzzy logic approach for the crane type selectin from the main crane types, which are mobile, tower, and derrick cranes. Linguistic information of crane types and dynamic/ static factors are translated into fuzzy relations. Then, aggregated importance weights are identified to select best crane that has the highest expected efficiency. Al-Hussein et al. [24] addressed the procedural algorithm for selecting and locating mobile cranes supported by databases such as crane lifting capacity charts, rigging equipment, and project information with graphical capabilities using MS-Visual Basic programming. Di el al. [25] suggested an mathematical algorithm for heavy lifts with lattice boom crane, which has more complex clearance issue due to the combination of boom and jib, that considers lifting capacity chart, geometrical constraint, and the ground bearing pressure incorporating in 3D modeling system. Olearczyk el al. [2] solved the crane selection problem by using optimized weighted distance, which considers the clearance of crane configuration such as swing tail, out rigger and boom. The crane operation components that are mathematically expressed by disaggregating enabled to implement the optimization algorithm easily in software languages for the full automation in the future.

After selecting the crane type and location, the feasibility of existing path has to be evaluated. With a popularity of module construction by mobile cranes in industrial projects, the importance of checking feasible path of the equipment becomes critical to avoid tedious work and inefficiency. Lei et al. [26] suggested automated path checking method that mapped the crane feasible operation range (CFOR) in each elevation based on the crane capacity, clearance, and site constraints to check with obstacle region. After that Lei el al. [5] discussed about the problem that requires crane walking path due to the far distance between pick location and set location. In this thesis, possible crane pick area and collision-free area are calculated to determine the walking path.

2.2.2   Mobile crane path planning algorithms and their comparison

Performance evaluation of path planning with 3 algorithms, which are Dijkstra, A* and GA, was completed with multi-objective approach of visibility, safety and transportation to check the effectiveness of algorithms to optimize the cost in construction sites regarding the path finding in the sites. A* tends to find more optimal solution than Dijkstra algorithm, but both are not producing efficient results in big scale problem. GA produced near-optimal solution with less computation time, but it is complicated to set up the process of search algorithm, and it provides less optimal solution than the other algorithms [10]. Also, Sivakumar el al. [27] applied GA for path planning of construction manipulators in a 2 DOF model.

Since heavy lifting operation can overcome their difficulties associated with maintenance problems regarding specialized equipment, transportation, availability, and tremendous cost by using cooperative cranes, Sivakumar el al. [11] suggested lift path planning algorithm with hill climbing and A* algorithm in the configuration space (C-space), which can represent high DOF environment effectively. Later, GA was used for exploring the near-optimized path planning of cooperative crane in an attempt to find a solution with less search time and cost [12]. The

performance was compared with heuristic search by Sivakumar el al. [11] in the C-space. To avoid the complexity of fitness formation and computation time, the author introduced dual fitness phases, which evaluates coordination and collision separately. The tests showed that the performance of GA was exceeding A *'s performance in terms of search time, and path cost calculated by module travelling distance; however, GA has limitation that it only generates the path with fixed number of configuration and, forming suitable fitness equation requires tremendous works. The results of hill climbing and A* algorithm was compared in the cases with synchronous and asynchronous movements. It showed that whenever there was a trapping space, hill climbing search tends to be trapped or take long detour to avoid obstacles because it only considered the neighbor node that has shortest distance to the set point. The results were evaluated with search time, number of movements, and the path cost. Even though A* took more time to search the feasible path than hill climbing, it generated more optimal and less costly path than hill climbing.

Cai el al. [4] proposed parallel genetic algorithm applying hybrid configuration concept to handle complex site condition. The optimization problem considered various costs such as energy cost, human cost and workability of operator while overcome collision and constrains of crane operation. The result was compared to GA algorithm in Ali et al. [12] after altering it into single crane problem from cooperative cranes problem. It shows that the results of proposed method require less operations, which decrease the human involvement, with stable convergence within fewer iterations.

Improved bidirectional RRTs algorithm was used to find an efficient lift path for a crawler crane [14]. This thesis considered mobility of cranes and nonholonomic kinematics to reflect real-world problem. By using a sampling strategy and expansion strategy, the paths are guided towards

the unexplored collision-free and high-quality space. This bidirectional RRTs method can provide the feasible result of crane path, which includes crane's turning, crane's travelling, slewing, luffing, and hoisting, quickly without collision

Han et al. [5] proposed an algorithm for automated path planning of the mobile crane, in which cases that requires crane's mobility to deliver modules at the set point. Furthermore, this crane walking path was visualized in *3ds Max* in an attempt to reduce planning time and cost [28]. Also, Han et al. [29] proposed 3D crane evaluation system to provide better operation and lift schedule by adding productivity that considers crane work cycle calculated by velocity of the movements, which is affected by safety factor at the location of lifted module,.

## 2.3   Path Planning Algorithms

### 2.3.1   Hill-climbing algorithm

Hill climbing belongs to local search that uses a mathematical optimization approach [30]. It starts from an arbitrary solution, then iterates to find a better solution by generating an incremental change each time. The incremental change is made until there are no further improvements in the solution. Hill climbing is easy to implement and fast to execute. However, It may converge and get stuck at local optima depend on the problem.

### 2.3.2   A * algorithm

A* was initially introduced by Hart et al. [31], which was an alternative of Dijkstra's algorithm [32]. This heuristic algorithm targets to find the smallest cost path from a start node to an end node with a following formula:

$$f(n) = g(n) + h(n) \tag{2-1}$$

Where g(n) is the cost from the start node to node n, h(n) is the expected cost from n node to the end node, and f(n) is the total cost of node n.

The algorithm starts with OPEN list which contains the start node and empty CLOSED list. Here, OPEN list contains generated nodes with heuristic function value, but not yet exanimated, and CLOSED list contains nodes already exanimated. Nodes in CLOSED list are kept in memory to check whether a new generated node was generated before. Until reaching to the end node, the best node in OPEN list, which is the node with the lowest f value, is examined. If the best node is equal to the end node, the algorithm terminates the process because it successes to find the solution. Otherwise, this best node is removed from OPEN list and saved in CLOSED list. Also, neighbor nodes of the best node are generated, and these new nodes are added in OPEN list if they are not already generated, which means they are not in CLOSED list. The node with the lowest f value will be picked and iterated the above procedure until reaching the end node or OPEN list is empty [30]. Fig. 1 shows the flowchart of A * algorithm.
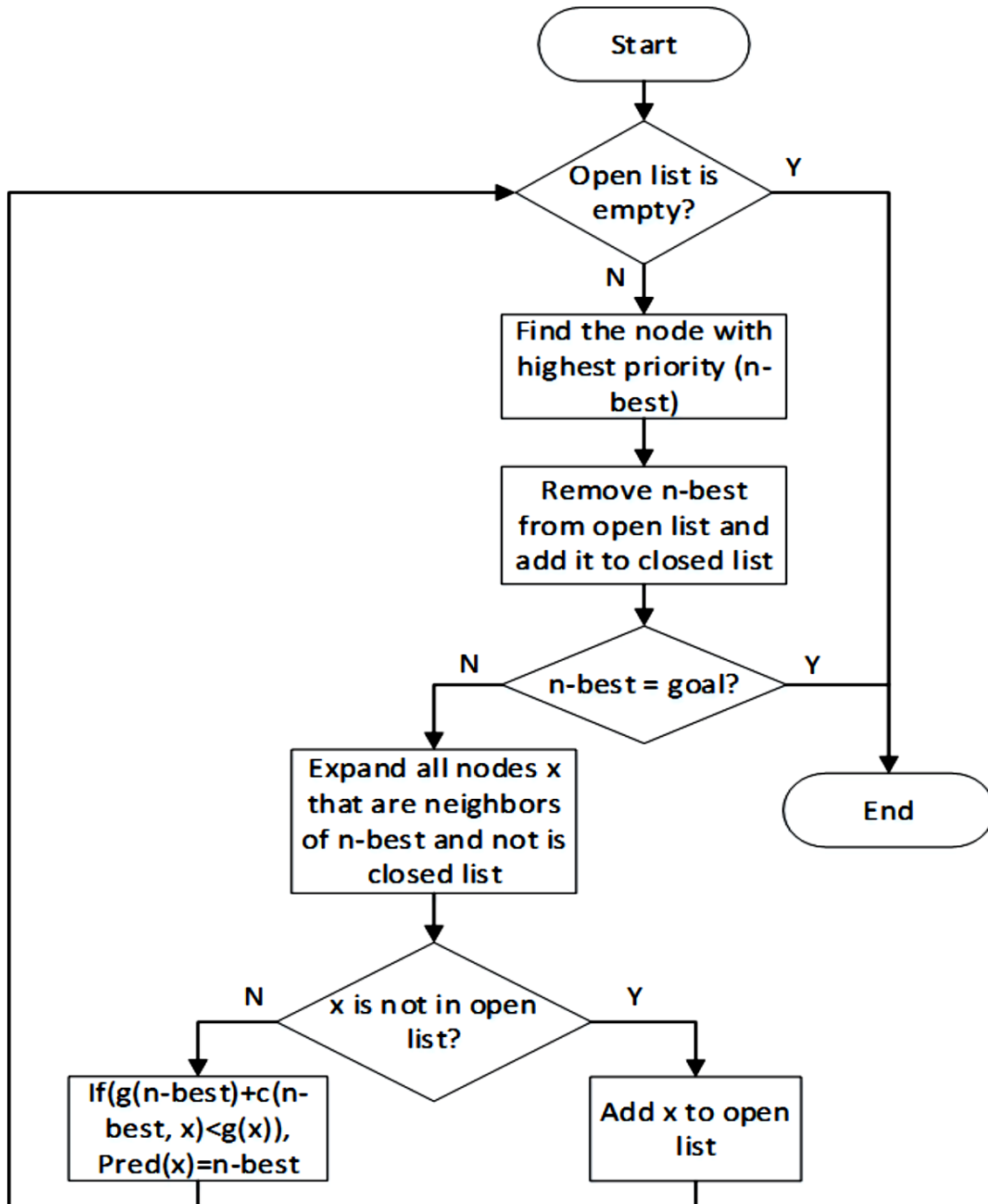
**Figure 1.** A* algorithm flowchart [33]

### 2.3.3 Rapidly-exploring Random Trees (RRT)

Rapidly-exploring Random Trees (RRT) was suggested by Lavalle [34] to solve nonholonomic path planning problem with high DOFs. It employs the randomized sampling strategy to extend the tree biased towards unsearched areas [35].
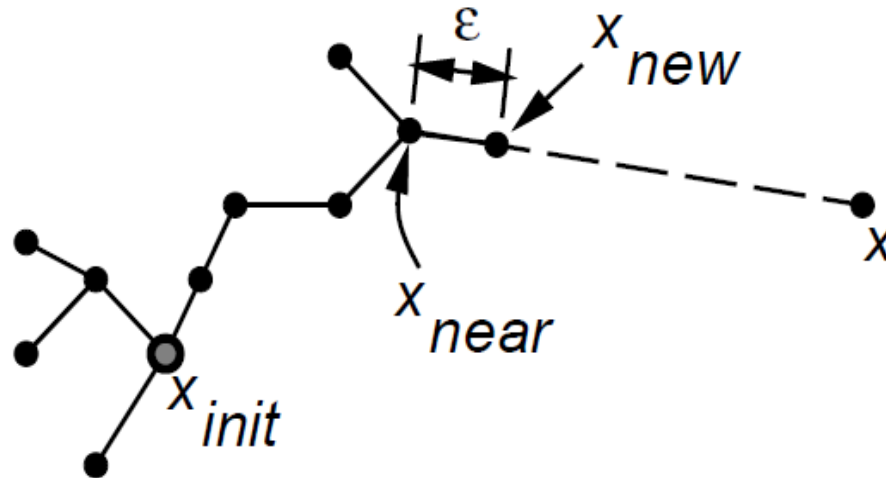


**Figure 2.** The EXPEND operation [36]

```
BuildRRT ()
  T. init (xinit);
  For k = 1 to K do
    xrand = Random_Configuration ();
    xnear = Nearest_Neighbor (xrand, T);
    xnew = Extend (xnear, xrand, Δq); Where Δq = incremental distance
    If (xnew =! null)
        T.Add (xnew);
  End
  Return T;
```

**Figure 3.** RRT pseudocode

As shown in Fig. 2, the tree incrementally expands by unit length rooted from initial configuration (x_init). The random configuration (x_rand) in the figure is uniformly sampled in the specified search area. The tree is extended towards the random configuration (x_rand) from the nearest configuration (x_near), in the existing tree. This process is repeated until the tree reaches to the predefined goal configuration. The growth of tree can be controlled by the sampling strategy to guide the exploring towards the goal. RRT has several advantages in terms of agility and efficiency mainly due to the randomness characteristic of the algorithm [15], [36]. Due to the randomness nature of RRT, the generated path tends to have zigzag pattern, which is not suitable for the practical crane operation that requires the short cycle path. Fig. 3 represents the pseudocode of the RRT algorithm.

### 2.3.4 Genetic algorithm

Genetic algorithm (GA) was first introduced by John Holland based on Darwin's theory of evolution, which is an evolutionary algorithm that is used for optimization and search problems. GA uses the concept of natural selection that has operators such as crossover, mutation and selection. In GA, solution candidates (individual) in a population is evolved towards the improved solution by evaluating each individual with the fitness, which is a function for the optimization. The individuals with better fit are selected to generate a next generation. The individual is consisted of members, called genome, that form the solution. After better individuals in a generation are randomly selected, the genomes in the individuals are randomly compounded and mutated to form a next generation. The whole process is iterated until the generation reaches maximum or the fitness value is satisfied [37]. Fig. 4 shows the flowchart of GA.
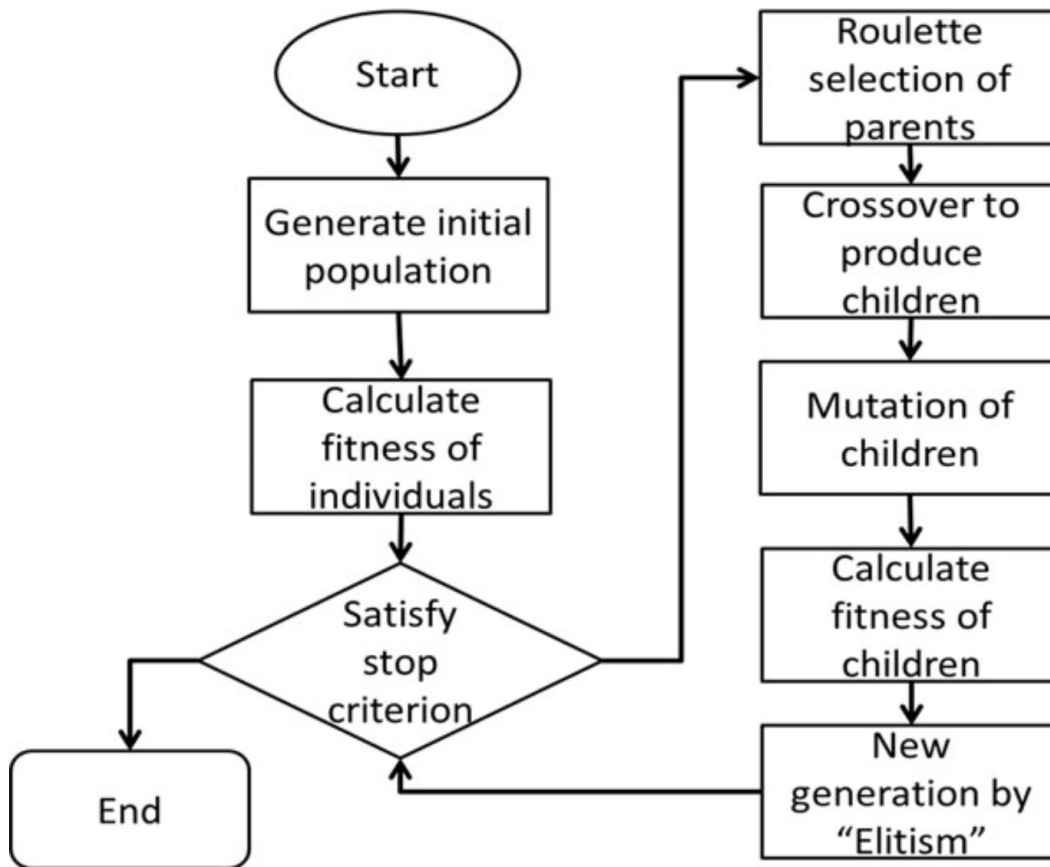
**Figure 4.** GA flowchart [38]

2.3.4.1 Initialization

The size of population depends on a characteristic of the problem. Most of time, the initial population is generated randomly to cover the entire search space for the possible solutions [37]. In previous researches [4, 12], the start and end configurations are fixed. Therefore, initial population is randomly generated by changing internal configurations within the bound values.

2.3.4.2 Selection

To breed a succeeding generation, individuals in the existing population are selected by a fitness function, where fitter individuals have more chance to be selected. The fitness function is defined according to a nature of problems to measure the quality of the solution. Defining fitness

function is challenging because it is hard to develop the fitness function that considers all the factors and their relation of the problem when the problem becomes complicated [37].

### 2.3.4.3   Genetic operators: Crossover and Mutation

After selecting parent individuals from the existing population, a set of new population is generated through generic operators: crossover, and mutation.

Crossover allows to combine genetic information of two parents to generate the new offspring, which has potential to be fitter than the parents since it is generated by selected individuals from the previous population. Depend on how to associate the genetic information from parent individuals, there are several popular crossover methods: single-point crossover, two-point and k-point crossover, and uniform crossover.

Mutation is used for the diversity of a population when it evolves to the next generation. Also, mutation prevents to have the offspring individuals too analogous to the parent individuals that could cause the local minima. Mutation alters the genetic information according to the mutation probability. If the mutation probability is set high value, the search will be close to a random search. Therefore, mutation probability is set as a low value in most cases [37].

### 2.3.4.4   Termination

The process above is iterated until the predefined number of generations is reached, satisfied solution is found, or any conditions that set in the algorithm are satisfied [37].

### 2.3.5   3D visualization-based mathematical algorithm (3DVMA)

3D visualization-based mathematical algorithm (3DMVA) which is an offline motion planning system introduced by Han at al.[28] for the efficient and safe design of collision-free mobile crane operations in congested sites. This thesis proposed a methodology based on two types

of interactive analyses using a mathematical algorithm and nature of 3D visualization using a centralizing project information which are: *(i)* rotation analysis is used to visualize 3D motions of the crane body configurations by calculating angles indicating the orientations of mechanical components in the crane system. These angles are calculated by the coordinates of the crane location and the pick point/set point of the lifted objects; and *(ii)* spatial analysis is used to design collision-free crane operations by inspecting the potential collision errors. The sufficient clearances between the obstacles and the crane body configurations are maintained and monitored to prevent potential collisions. This method is beneficial for the dynamic design changes and automated design of collision-free 3D-based motions of crane operation. As a result, it supports lifting schedules and site layouts in terms of the safety, quality, and time saving.

## 2.4   Limitation of Previous Research

According to the literature review, algorithms for the lift path planning of the mobile crane have been introduced and the results were compared in the construction industry. However, there are several limitations from the previous research as follows:

1) Previous works didn't fully apply the realistic crane mobility (i.e. step resolution, and the safety factor). For example, due to the low step resolution for swing, luffing, and hoisting which 10 °, 5 °, and 2 ft units respectively, the path results didn't reflect the realistic solution of crane operation.

2) The practical site environments (i.e., congested and dynamic site layout changes due to the lifting schedule and obstacle environment) were not sufficiently implemented in the methodology and case study.

3) The comprehensive comparison that considers the multi-factor measurement and site constraints are not done yet. For example, the comparison of previous works was limited to computation time, and travel distance of lifted objects, which doesn't fully evaluate the quality of path.

# Chapter 3:    METHODOLOGY

The objective of the crane lift path planning is to find collision-free sequences of crane motions based on various pick and set positions on a site while overcoming the limitations of previous works. There are several requirements which should be satisfied in order to be considered as a feasible path reflecting the practical rules and the natural mobility of the crane lifts: *(i)* the crane configurations should be moved based on the kinematics constraints of the configurations represented as degree of freedoms (DOF) in the permissible range; *(ii)* the crane lift paths must be collision-free among the lifted object and obstacles already installed; *(iii)* the total weight of the lifted object should not exceed the allowable crane capacity that is provided by a manufacturer's capacity chart; and *(iv)* dynamic site layout should be reflected in accordance with scheduled sequences of the selected objects. It should be noted that this thesis considers only lattice-boom mobile cranes mounted with superlift which is mainly adopted in heavy industrial projects that require high capacity to lift heavy modules and facility elements (e.g., vessels).

## 3.1   Configuration space and Degree of freedom

Configuration space (C-space) was started form the idea to present the manipulator's configuration to a point by Udupa [39], then it was introduced to plan collision-free paths by Lozano-Pérez [40]. C-space has several benefits comparing to real space when it comes to solve the path finding problem. In real space, the dimensions are limited to the Cartesian space which has X, Y, Z coordinates; However, in C-space, each DOF of manipulator becomes an axis that means each configuration of manipulator can be presented as a point in C-space [11]. Due to the high DOF in mobile crane as shown in Fig. 5, representing crane configuration using C-space concept with active DOFs will be beneficial to solve the path planning problem. Fig. 5 described

7 DOFs in mobile crane as following: swing, luffing, hoisting, hook rotating, boom extension, turning, and travelling.
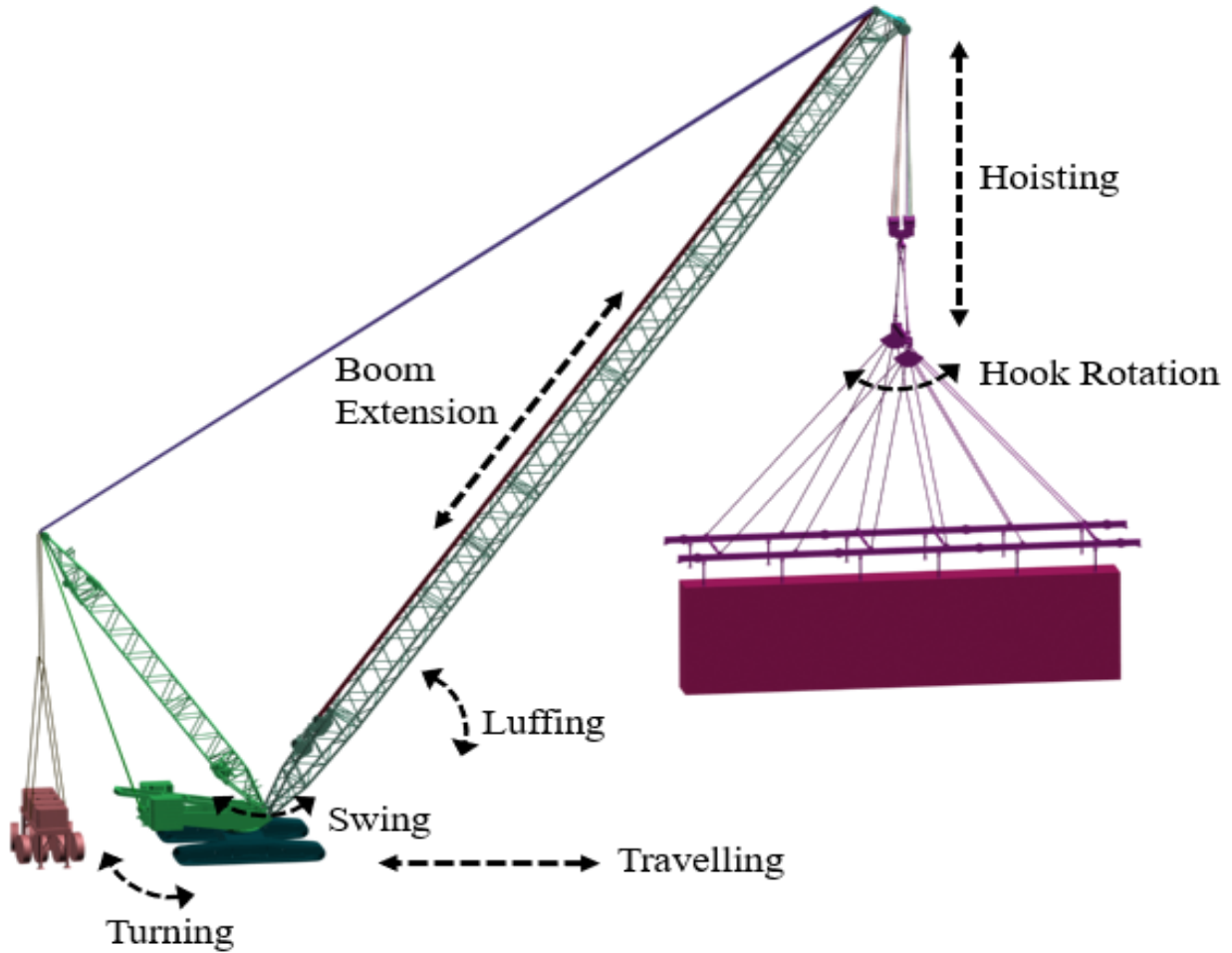


**Figure 5.** DOF of lattice-boom mobile crane configurations

Based on the consideration of constrains (e.g., obstacles and crane capacity) which do not allow the mobility of the crane (e.g., swing, luffing, and hoisting), there are two types of crane operations: *(i)* pick from fixed operation (PFP), which completes all lifts on one single location; and *(ii)* pick and walk operation (PWO), which includes turning and travelling as parts of active DOFs. The scope of this thesis considers the lifting method with PFP, which is usually preferred from the practitioner's perspective since it minimizes collision errors and crane capacity issues (e.g., required capacity exceeds the allowable capacity) [28]. In addition, hook rotation and boom

extension are practically not allowed during the crane operations. Accordingly, the mobile crane mainly is operated by three active DOFs, which involve swing ($\alpha_{swing}$), luffing ($\alpha_{luffing}$), and hoisting ($l_{hoisting}$). In this respect, the configuration of one single crane motion (CCM) used in this thesis to implement algorithms is expressed as Eq. (3-1) and Eq. (3-2).

$$P_j = \{C_i\}_{i=0,1,\dots,n-1} \tag{3-1}$$

$$C_i = (\alpha_{swing}, \alpha_{luffing}, l_{hoisting}) \tag{3-2}$$

It is also noted that the increment value to search for swing, luffing, and hoisting is 1°, 1°, and 1 ft, respectively, to reflect a high step resolution that considers the realistic crane mobility. For example, when the configuration of current crane motion ($\alpha_{swing}, \alpha_{luffing}, l_{hoisting}$) was examined to form one of crane motions in a path with a corresponding search method, six neighboring CCM ($\alpha_{swing} - 1, \alpha_{luffing}, l_{hoisting}$), ($\alpha_{swing} + 1, \alpha_{luffing}, l_{hoisting}$), ($\alpha_{swing}, \alpha_{luffing} - 1, l_{hoisting}$), ($\alpha_{swing}, \alpha_{luffing} + 1, l_{hoisting}$), ($\alpha_{swing}, \alpha_{luffing}, l_{hoisting} - 1$), ($\alpha_{swing}, \alpha_{luffing}, l_{hoisting} + 1$) are created to search the optimal crane lift path.

## 3.2 Problem Structure
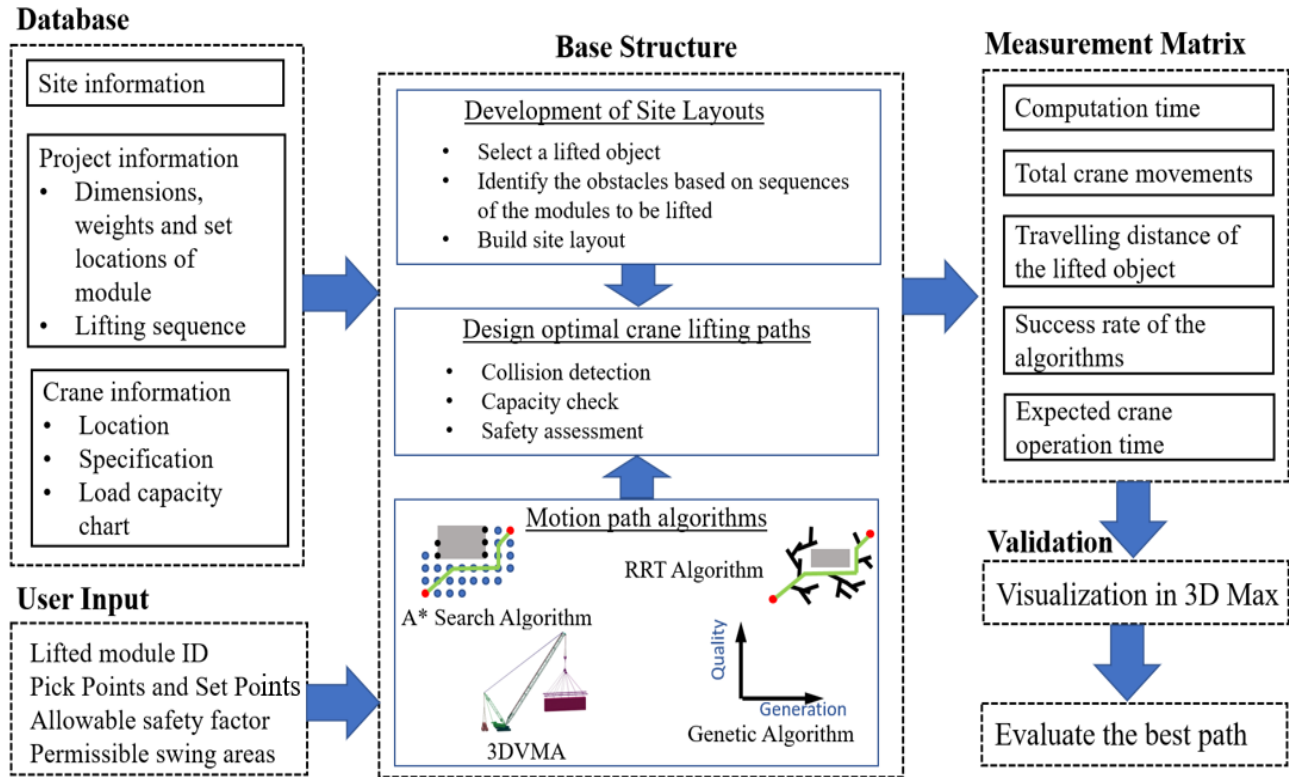


**Figure 6.** Proposed Methodology

In order to apply multiple algorithms in the specified problem, it is mandatory to set up the base structure for a reasonable comparison and flexible implementation. Fig. 6. illustrates the proposed methodology for the comparison of the lift path algorithms. The database consists of: *(i)* site information, *(ii)* project information such as dimensions, weights and set locations of the modules, sequences of the modules to be lifted, and the size of the site; and *(iii)* the crane information including the type of the mobile crane, capacity chart, dimensions of crane configurations (e.g., boom length) and dimensions and weights of the rigging. In order to apply multiple lifting path searching algorithms, this thesis develops a base structure which facilitates the comparisons of various algorithms in the same environment and constraints. The base structure consists of: (*i*) selecting the object to be lifted; (*ii*) developing the obstacle environment (i.e., site

layout) by importing the project information from the database. According to the sequence of lifted module, previously installed objects become obstacles for the current lifted module; (*iii*) searching for optimal lift paths using algorithms with A* algorithm, RRT algorithm, GA, and 3DVMA based on assessing the crane capacity, safety factor, and collision detection described in the next section for detail information; (*iv*) extracting the results by implementing measurement metrics which are consist of computation time, total crane movements, travelling distance of the lifted object, success rate of the algorithms, and the expected cane operation time; and (*v*) visualizing results of lift paths for validation in 3D Max. The proposed methodology in implemented in a Visual Studio Code environment with Python, and Matplotlib is used to plot the lift paths of each algorithms promptly.

## 3.3 Crane capacity assessment

40% of the mobile crane accidents [3] are related to crane collapse which can be occurred mainly by the capacity failure and incorrect crane support design. To prevent the crane capacity failure, it is important to assess the crane load capacity and the safety factor to perform the safe crane operation prior to the actual lifting.

Crane capacity and safety factor are evaluated by calculating of the required lifting weight ($W_{Total}$) and the working radius ($R_A$) expressed in Eq. (3-3, 3-4, 3-5), and Fig. 7 shows the crane configurations of active DOF. The safety factor is calculated by $W_{Total}$ and the gross capacity (GC) at allowable crane working radius ($R_L$) which are obtained from the capacity chart provided by the crane manufacturers. This safety factor is also used to calculate the expected crane operation times (cycle time) of paths which are computed based on the speeds of the crane motions determined by the safety factors: the lower safety factor results in higher speed and the higher safety factor results in slower speed. To ensure the realism of the lifting planning, the preparation time (i.e., time lag among swing, luffing, and hoisting) is incorporated by applying penalty time

23

matrix with the intention that: if there is a change of motion types in the lifting process, a penalty is applied. Therefore, the path results reflect the realistic outcomes that can be applied into the actual project. The penalty time matrix of crane operation and the detail descriptions of calculating crane operation time is referred to Han et al. [26].

$$GC \geq W_{Total} = W_{Lifted} + W_{Hook} + W_{Sling} + W_{Spreadbar} \qquad (3\text{-}3)$$

$$R_L \geq R_A \qquad (3\text{-}4)$$

$$\text{Safety factor } (\%) = \frac{W_{Total}}{GC} \times 100 \qquad (3\text{-}5)$$

Where GC = gross capacity from the database; $W_{Total}$ = total weight; $W_{Lifted}$ = lifted object weight; $W_{Hook}$ = hook weight; $W_{Sling}$ = sling weight; $W_{Spreadbor}$ = spreadbar weight; $W_{Hoist}$ = hoist weight; $R_L$ = allowable crane working radius; and $R_A$ = required working radius from a crane center point to a lifted object center point.
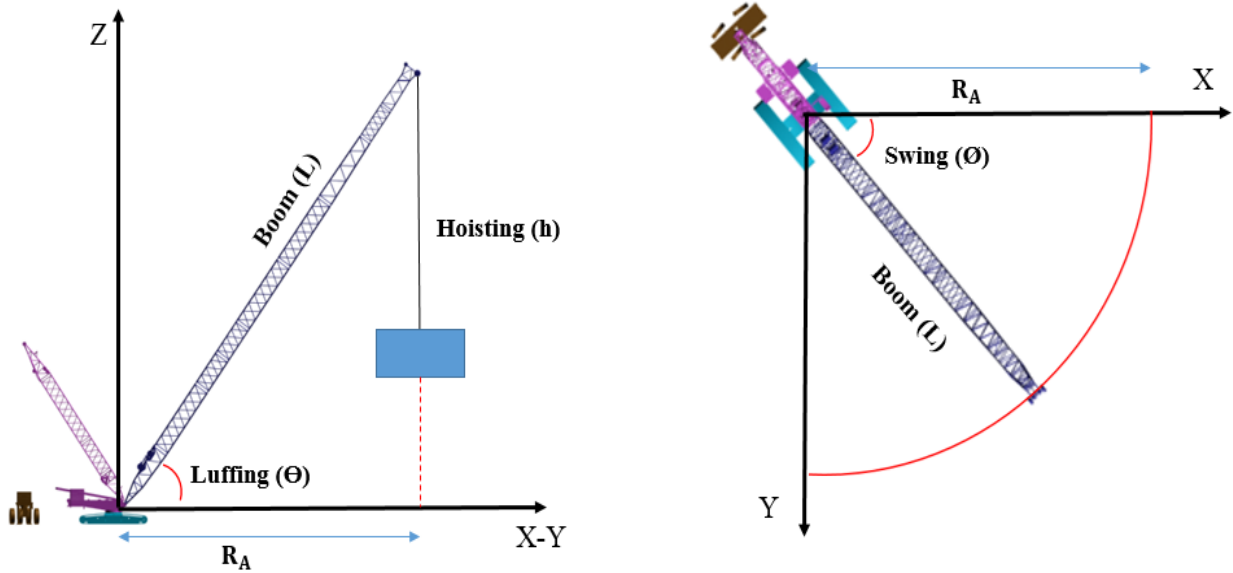


**Figure 7.** Crane configurations of active DOF

In this thesis, from the module ID of the lifted object, the information such as total lifting weight ($W_{Total}$) which is a sum of the lifted object's weight and corresponding rigging system

weight, coordinates of pick position based on the center point of lifted object, and initial crane configuration at the pick position are obtained. Therefore, obtained $W_{Total}$ can be compared with GC in the lifting capacity chart in the database using Eq. (3-3). Since the proposed algorithms generate the concatenated crane motions as the result, interrelated coordinates should be calculated upon the change of the crane motions. The Cartesian coordinates (x, y, z) at current crane configuration are obtained by Eq. (3-6).

$$R_A = L \, \cos\theta$$
$$x = R_A \cos\emptyset$$
$$y = R_A \sin\emptyset$$
$$z = L \sin\theta - h$$

(3-6)

Where L = boom length; $\Theta$ = luffing angle (degree), $\emptyset$ = swing angle (degree), $R_A$ = distance between crane center point and lifted object center point; and h = hoist length (ft). This (x, y, z) coordinates are based on the center point of lifted object and the pivot point of the crane. Once $R_A$ had been decided upon, it is compared with $R_L$ as Eq. (3-4) for the crane capacity assessment. Following this, GC and $W_{Total}$ are used to calculate the safety factor at current configuration using Eq. (3-5).

Commonly, safety factor between 85 % to 90 % is set to the upper limit depend on the company's safety regulation. Safety factor between 90 % to 95 % is acceptable under the lift engineer's supervision while more than 95 % of safety factor is unacceptable [29]. In this thesis, the crane operation with the safety factor exceeding 85% is considered as unsafe operation. Hence,

the crane configuration within the allowable working radius and safety factor of 85 % is considered as safe operation.

The safety factor is not solely used to identify the safety of operation; however, it is also used to calculate the operation time of path by indicating the speed of the motion depending on the corresponding safety factor. Since the slewing and hoist speeds (S) that provided by manufacturer are maximum values, the allowable minimum ($P_{min}$) and maximum ($P_{max}$) percentages defined by users based on company's regulation are used to present a distribution of speed range. Thus, the accepted speeds range distribution is calculated by Eq. (3-7) and shown in Fig. 5 when the minimum ($F_{min}$) and maximum ($F_{max}$) safety factor is 0% and 100%, respectively. In this thesis, $P_{min}$ = 20 % and $P_{max}$ = 60% are applied.

$$V_{slewing\ max}(°/min) = (P_{max} \times 0.01) \times S_{slew} \times 360°$$

$$and\ V_{hoisting\ max}(ft/min) = (P_{max} \times 0.01) \times S_{hoist} \times 360°$$

$$V_{slewing\ min}(°/min) = (P_{min} \times 0.01) \times S_{slew} \times 360°$$

$$and\ V_{hoisting\ min}(ft/min) = (P_{min} \times 0.01) \times S_{hoist} \times 360°$$

(3-7)
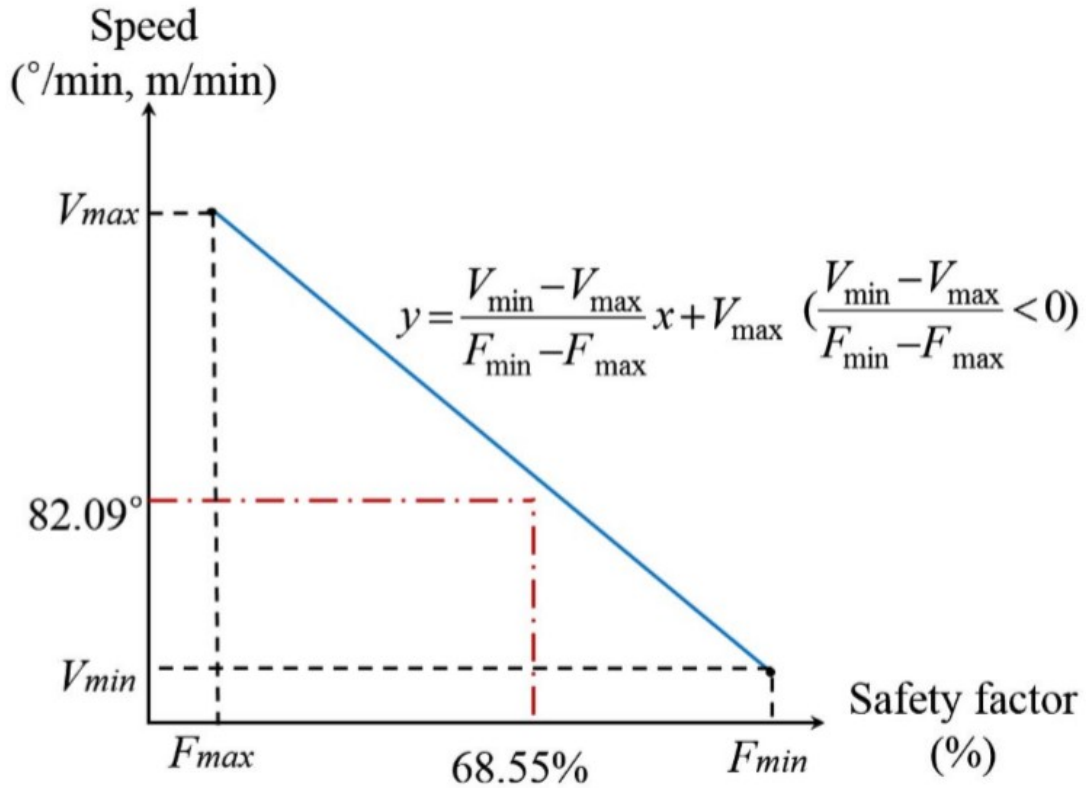
**Figure 8.** Interval range of speeds [29]

$$y = \frac{V_{min} - V_{max}}{F_{min} - F_{max}} x + V_{max} \ (°/min, m/min) \ (\frac{V_{min} - V_{max}}{F_{min} - F_{max}} < 0) \qquad (3\text{-}8)$$

As shown in the Fig. 8, the speed of motion is influenced by the safety factor as higher speed at lower safety factor and vice versa. The corresponding speed at safety factor is calculated by Eq. (3-8) from the variation diagram Fig. 8. This calculated speed is used to obtain the operation time of crane operation; however, to reflect the realistic analysis, preparation time to convert the crane motions has to be considered. To reflect this, the modified time penalty matrix of crane movements are applied as shown in Fig. 9 [29]. When the motion is changed, the extra penalty time is added based on the time penalty matrix. For example, if the crane motion is changed from

rotation (e.g., swing) to boom up or down, 0.75 minute is added up as a penalty time as a consequence of the motion change. At the end, the cycle time for the module lifting operation will be the sum of operation time and the time penalties.

| Crane motion | Boom up or down | Rotate (Arc) | Hoist up | Hoist down |
|---|---|---|---|---|
| Boom up or down | 0.00 | 0.75 | 1.00 | 0.50 |
| Rotate (Arc) | 0.75 | 0.00 | 0.50 | 0.75 |
| Hoist up | 0.75 | 1.00 | 0.00 | 0.00 |
| Hoist down | 0.50 | 0.75 | 0.00 | 0.00 |
| Walking | | 2.00 | | |

Note: Unit = minute.

**Figure 9.** Time penalty matrix [29]

## 3.4 Collision Detection

During mobile crane operations, there are three types of the potential collision: *(i)* type 1: between the crane configurations and obstacles represented in Fig. 10(a); *(ii)* type 2: between the crane configurations (mostly boom) and the lifted object shown in Fig. 10(b); and *(iii)* type 3: between the lifted object and obstacles illustrated in Fig. 10(b). Type 1 collision is prevented by the allowable permissible range of superstructure swing angle determined by a minimum superstructure swing angle ($S_{min}$) and a maximum superstructure swing angle ($S_{max}$) as shown in Fig. 3(a). Type 2 collision is prevented by limiting the hoisting length with a consideration of the clearance between the boom and the lifted object as shown in Fig. 3(b). The corresponding equation to calculate the hoisting range is expressed in Eq. (3-9, 3-10).
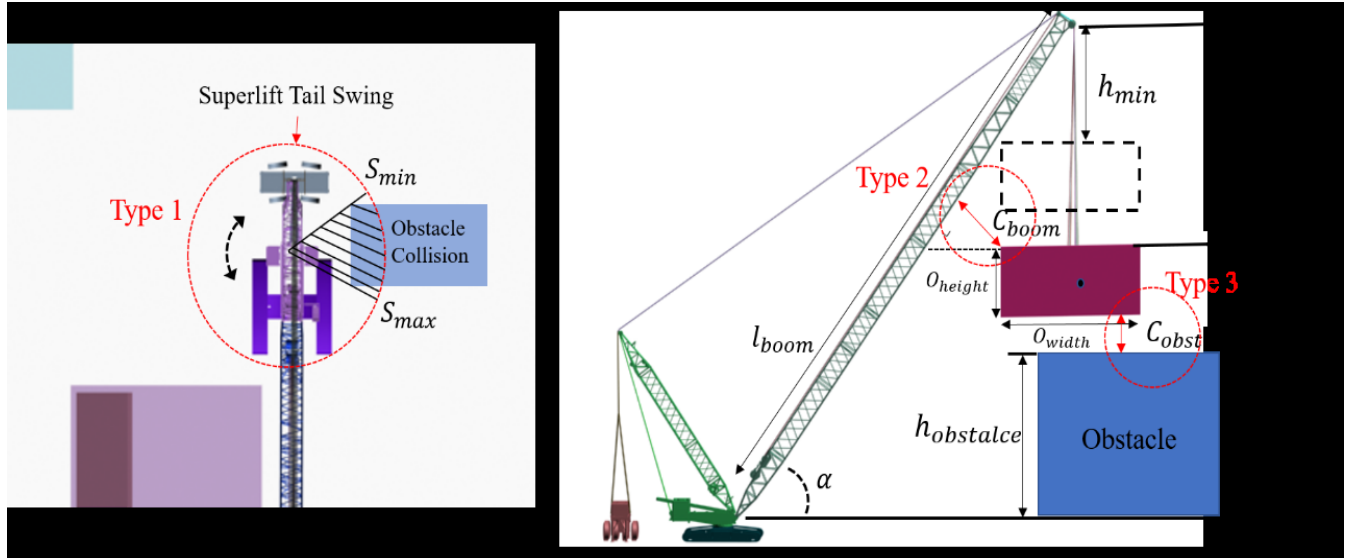
(a) Type 1                                        (b) Type 2 and Type 3

**Figure 10.** Three types of potential collisions

$$h_{min} = (\frac{C_{boom}}{\sin(L_{min})} + \frac{O_{width}}{2}) \tan(L_{min}) \qquad (3\text{-}9)$$

$$h_{max} = (l_{boom} \sin(L_{max})) - O_{height} - C_{obstacle} \qquad (3\text{-}10)$$

Where $h_{min}$ = the minimum hoisting length; $C_{boom}$ = allowable clearance between the boom and the lifted object defined by users; $C_{obstacle}$ = allowable clearance between the lifted object and existing obstacles defined by users; $L_{min}$ = the minimum luffing angle; $O_{width}$ = the width of the lifted object; $h_{max}$ = the maximum hoisting length; $h$ = the vertical distance between boom top to the ground level; $L_{max}$ = the maximum luffing angle; $l_{boom}$ = the length of the boom given by the crane information; $h_{obstacle}$ = the height of the obstacle; and $O_{height}$ = the height of the lifted object. Here, $L_{min}$ and $L_{max}$ are given by the manufactures. $L_{min}$ and $L_{max}$ are determined by minimum and maximum working radii from a crane capacity table provided by a crane manufacturer and $l_{boom}$. In this thesis, the allowable clearances between the boom, existing obstacles and lifted object are defined as 2.5 ft, respectively.

29

Type 3 collision is solely monitored in the algorithms under the conditions which are: *(i)* the lifted object does not rotate during the operation; and *(ii)* in a practical view, the boom and the lifted objects are always at a perpendicular position during the crane operation instead of parallel position. Based on the geometry arrays of the objects, collisions can be detected by identifying the interruption between the lifted object and obstacles in the coordinate system by comparing minimum and maximum x, y, and z coordinates of the modules and existing obstacles, which are the previously installed objects.

It should be noted that all modules are presented as rectangular shape in this thesis. In a top-down plane view, each corner of the lifted object (LO) and existing obstacle (EO) has *x, y,* and *z* coordinates during the entire lift path. To describe the example of collision detection efficiently, *x* coordinates of LO and EO are expressed as Min (LOx), Max (LOx), Min (EOx), and Max (EOx), respectively. As shown in Fig. 11(b) and (c), collision can be occurred when Max (LOx) is smaller than Max (EOx) and Max (LOx) is greater than Min (EOx). Otherwise, current motion of the lifting path has no collision as represented in Fig. 11(a) and (d). To have collision detection in 3D environment, the algorithms also apply this method into *y* and *z* dimensions, respectively. Fig. 12 represents the pseudo code which represents the process flow of a 3D collision detection method.

The value of the clearance is considered at the minimum and maximum coordinates in each dimension of the lifted object to ensure the safe operation. Based on the sequences of the module installation in the database, some modules, which the sequences of them are earlier than the sequence of the lifted object, become existing obstacles if these obstacles are in the crane maximum radius. For example, if a module is lifted with sequencing number 10, the modules with sequencing number 1 to 9 will be considered as potential obstacles. If these potential obstacles are located within the crane maximum radius at the current crane position, those are loaded as the actual obstacles and they are used for the collision detection.
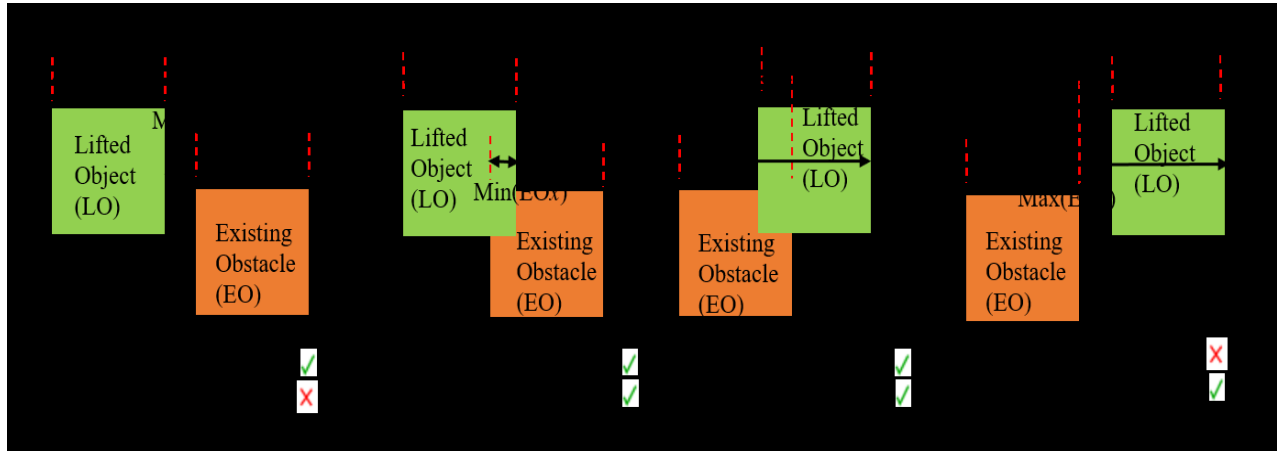


**Figure 11.** Examples of the collision identification in x axis

```
S: set of all modules in a project
LO: lifted object
O: [ ] /*Empty list*/
/* Identification of the existing obstacles*/
For each module M in S do:
  If (sequence of M < sequence of LO):
      If M is within the crane working radius:
          Append M to O
/* Collision detection*/
For each obstacle EO in O do:
  If min(LOx) < max(EOx) and max(LOx) > min(EOx),
    min(LOy) < max(EOy) and max(LOy) > min(EOy) and
    min(LOz) < max(EOz) and max(LOz) > min(EOz) :
    Collision = True
  End if
```

**Figure 12.** Pseudo code and for the process flow of the collision detection

## 3.5  Algorithms Development

3.5.1   A * algorithm

The A* search is a heuristic algorithm to find the lowest "cost" path which is a minimum travel distance from a start node to an end node expressed as Eq. (3-11):

$$f(n) = g(n) + h(n) \qquad (3\text{-}11)$$

Where g(n) is the cost of the path from the start node to the $n^{th}$ node, h(n) is the heuristic function that estimates the cost of the cheapest path from the $n^{th}$ node to the goal node, and f(n) is the total cost of the path.

A* search algorithm initially defines the start and end nodes which are the pick CCM and set CCM, respectively. This algorithm initializes to create two lists: *(i)* OPEN list involves pick CCM and expanded nodes which are not yet used to generate the neighboring nodes to identify optimal lift paths; and *(ii)* an empty CLOSED includes the nodes which are the best nodes identified by the lowest f(n) among the nodes in OPEN list. Once the best node moves to CLOSED list, it is removed from OPEN list to prevent repetitive works with the same nodes. When the best node in CLOSED list is not the same as the end node, the neighboring nodes are generated to expand search areas around the best node since A* algorithm does not find out a crane lift path yet.

These neighboring nodes must satisfy the requirements: *(i)* the CCMs of the neighboring nodes are within the permissible range of the superstructure swing angle, collision-free and safety factor is less than 85%; *(ii)* the nodes must not be the same as ones in the CLOSED list; and *(iii)* when the CCM is the same, g(n) of the neighboring node must be less than g(n) of an existing node in OPEN list because it is efficient to only consider the less costly node. Once the new nodes satisfy these requirements, they are involved in OPEN list and the same procedure is repeated until the best node reaches to the end node. At this junction, it should be noted that the requirement *(iii)* is essential to not only prevent excessive calculations of f(n) by minimizing the number of nodes in OPEN list but also reduce the computation time of the algorithm to identify the optimal crane lift path. When the best node reaches to the end node, the algorithm traces back the parent nodes in order to present the entire lift path for a lifted object. Fig. 13 represents the flowchart of the A* algorithm used in this thesis.
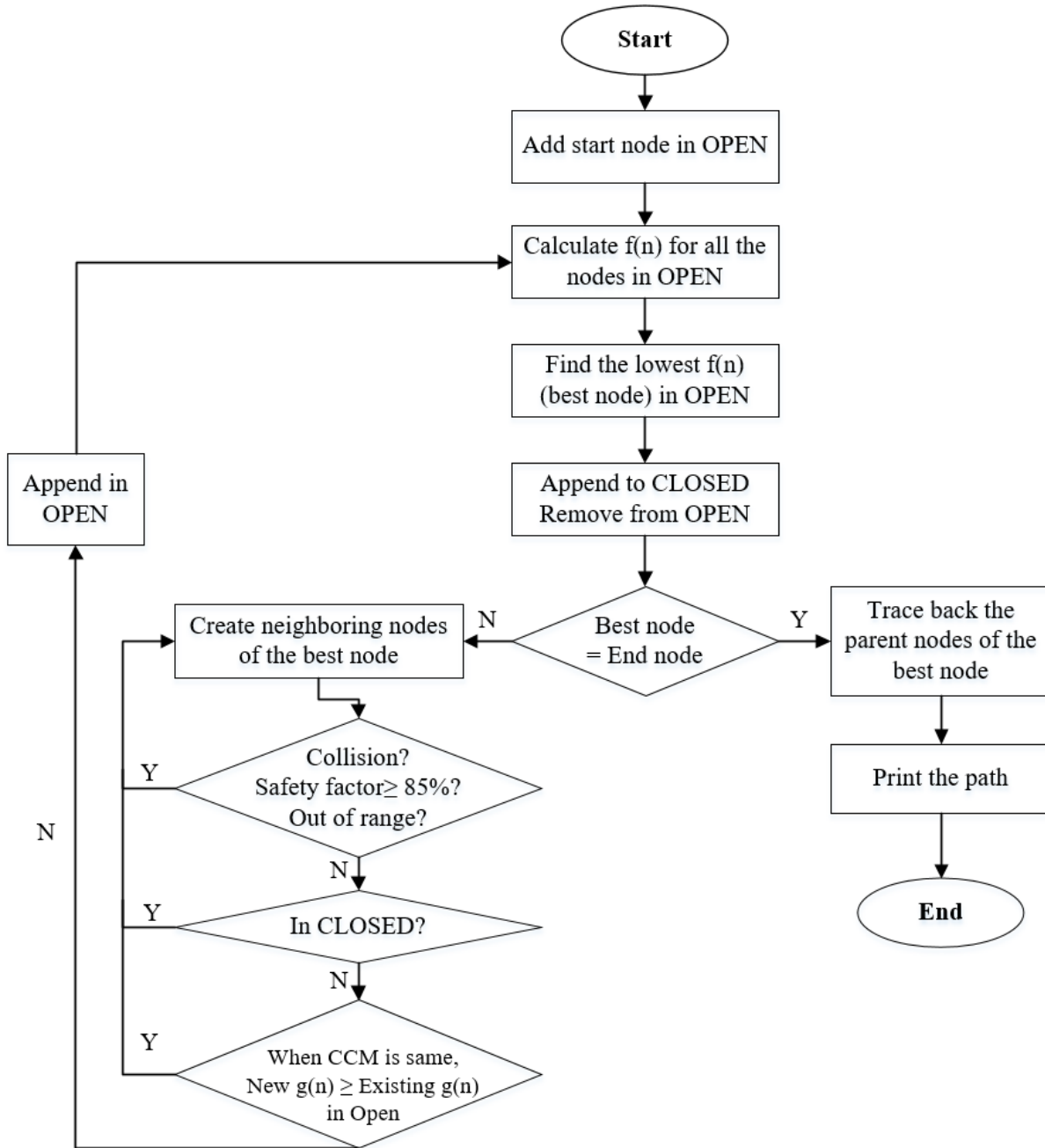
**Figure 13.** Flowchart of A* Search

### 3.5.2 Rapidly exploring Random Trees (RRT)

Rapidly-exploring Random Trees (RRT) is initially suggested by Lavalle [34] to solve nonholonomic path planning problem with high DOFs. It employs the randomized sampling strategy to extend the tree biased towards unsearched areas in order to find out a lift path [35].

The flowchart of RRT algorithm used in this thesis is represented in Fig. 14. A tree is initiated by adding the start node in the node list, then it is expanded by one unit of each crane motions based on the sampling strategy which provides to improve the quality of the lift path and the efficiency of the algorithm.

The sampling strategy have a key role to control the direction of the tree growth to find the optimal path with the prevention of collision and local confinement [14]. In this thesis, sample rate ($p$) is used to get the random sample configuration (RSC). In this respect, there are two types of the RSC: *(i)* the tree expands toward the end node when the RSC is the end node represented as CCM with the probability of the sample rate; and *(ii)* with the probability of (100- $p$), the RSC is the random CCM, which must be in the permissible range of the crane configurations and the tree expands randomly within the unsearched areas. Previous research recommends 5% to 10% as $p$ to bias towards the end node [41]. Otherwise, 100% of probability possibly gets the node stuck by failing to avoid obstacles. In this respect, this thesis uses 10% as sample rate.

To determine the direction of expanding the tree, the nearest node to RSC is obtained from the node list (existing tree). Based on the location of the nearest node, the neighboring nodes are generated and one of them is selected by two methods: *(i)* identification of a node which has a minimum distance between neighboring node and RSC; and *(ii)* the node that has the smallest difference of CCM values comparing to the CCM of the RSC. Both methods are implemented in the case study and compared to verify which one results in a better path solution based on the consideration of the measurement metric described below.

After selecting the node candidate to expand the tree, the collision detection and safety factor assessment are implemented. When the node candidate does not meet the requirements, which means detected collision and the safety factor less than 85%, the sampling process is

repeated. Otherwise, the node candidate becomes one of the expanded nodes which is connected to find out the optimal crane lift path. Furthermore, when the expanded node reaches to the end node, the path is printed by tracing back the parent nodes that saved in the node information. If the expanded node is not equal to the end node, it is added to the tree and the same procedure is repeated from sampling nodes until it reaches the end node.
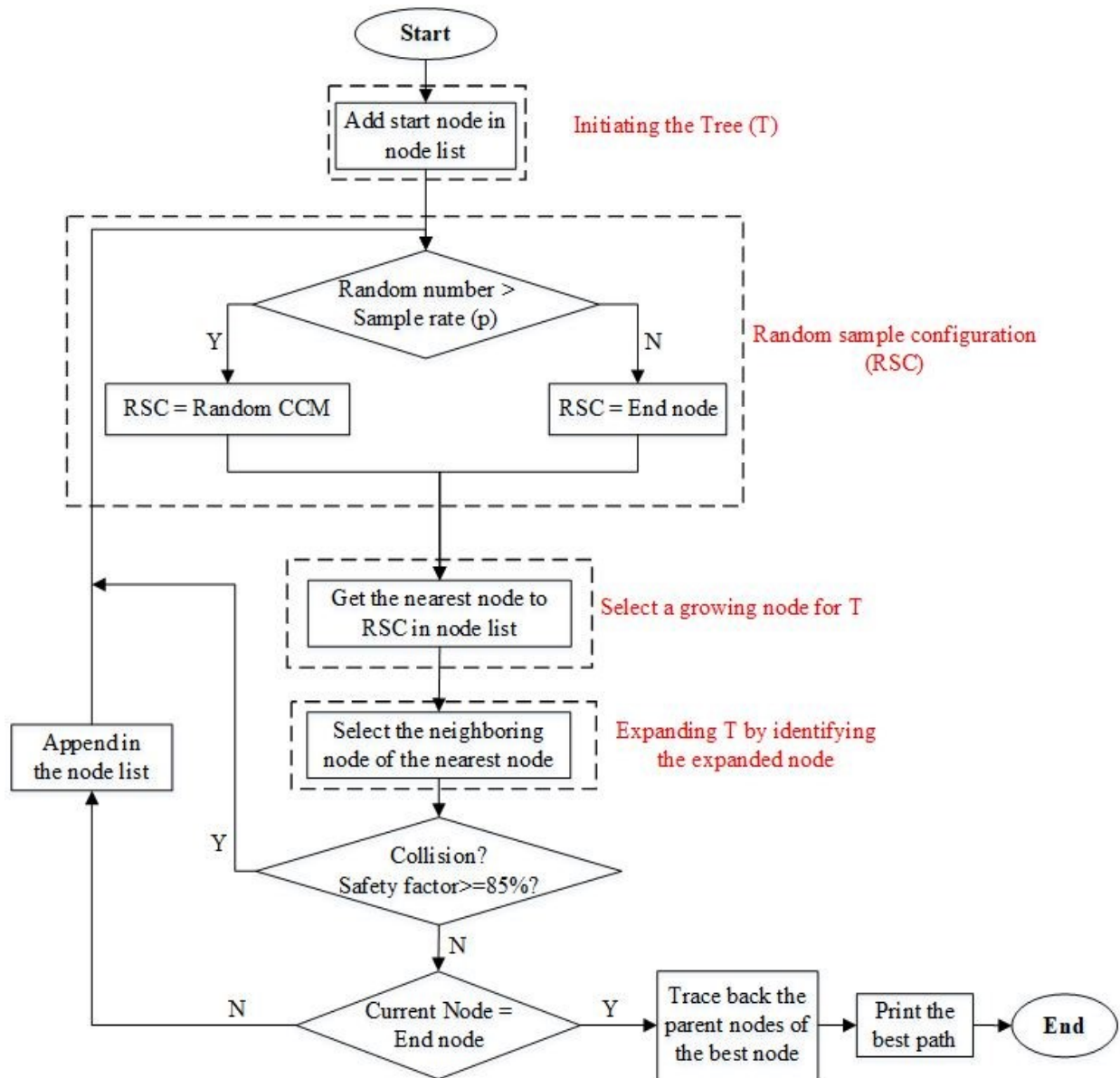


**Figure 14**. Flowchart of RRT

36

### 3.5.3 Genetic Algorithm

The genetic algorithm (GA) is an evolutionary algorithm which is mainly used for optimization and search problems in various domains including construction. GA uses a concept of natural selection using genetic operators such as selection, crossover, and mutation. In GA, a population consisting of solution candidates (individuals) is evolved towards the improved

**GA Input**

Size of populations (P), generations (G), rate of crossover (Rc), rate of mutation (Rm), maximum number of CCM (Cm), maximum number of crane movements (Mm), scaling factors ($\lambda 1$, $\lambda 2$),Percentage of the best individuals (Pbest)

**GA Process**

Initial Population

Call Fitness Evaluation

# of generation = G?

Y

Print the best path

N

Selection

Crossover

Mutation

End
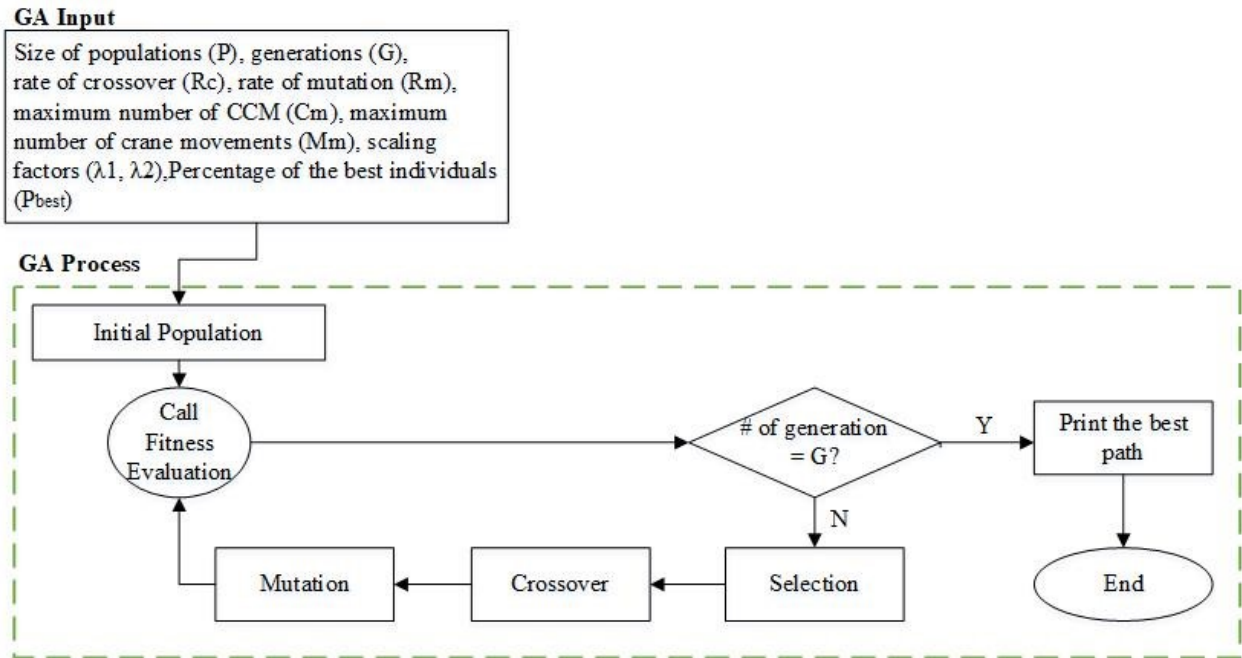
**Figure 15.** Flowchart of GA

solution by evaluating each of individuals with a fitness function for the optimization by generation. Since the fitness function assigns fitness scores to individuals, it is mainly used to select the fittest individuals in the population for a next generation. The main process flow of GA is represented in Fig. 15.

3.5.3.1   Initial Population and Fitness Evaluation

An initial population of paths is randomly built by satisfying one constraint which is the permissible range of crane configurations. For example, if population is set as 100 by a user, 100 individuals (crane lift paths) are created randomly for one generation. Then, each of individuals in this population is evaluated by the fitness function as represented in Fig. 16.
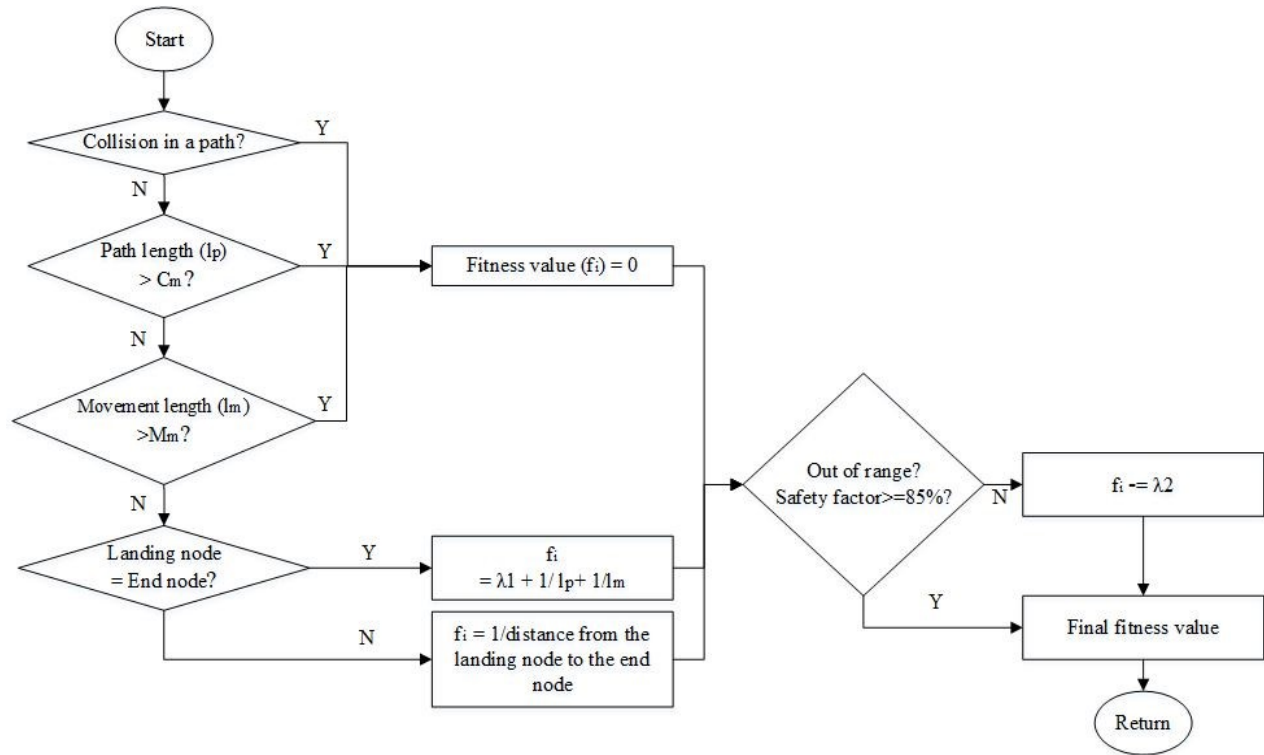


**Figure 16.** Process flow of fitness evaluation

The fitness evaluation has a critical role in GA which improves the quality of paths by identifying the constraints of crane operation such as collisions, permissible range, and safety factor which are defined by a user. In this thesis, higher fitness value indicates more suitable solution for the problem. To implement the fitness evaluation, there are a few evaluation setting values: maximum number of crane motions ($M_m$), and maximum number of CCM ($C_m$). These values are used to not only prevent unlimited generations of the paths but also search for the practical and optimal crane lift paths. At this junction, it should be noted that minimum numbers

38

of crane motion changes are preferred in practice for safety and productivity improvement. Based on these evaluation setting values, the fitness value ($f_i$) represents the suitability of the paths. That is, when the path does not satisfy the evaluation setting values or collision is detected in the path, $f_i$ is 0. It should be noted that the number of crane motions counts on the number of CCM grouped by the same crane motion such as swinging, luffing or hoisting. For example, a part of the CCM in the path is (10, 10, 10), (11, 10, 10), (12, 10, 10), (13, 10, 10), and (14, 10, 10) in accordance with the increment value by one unit described in previous section. In this respect, the number of CCM is five but the number of crane motions is only one since the crane swings from 10° to 14°.

As shown in Fig.16, if there are any violation in three requirements, which are collision, number of CCM, and number of crane motions, $f_i$ becomes 0. if the path has no violation in three requirements, the last landing node of the path is identified whether it arrives at the end node which is the set CCM of the lifted object. When it is landed at the end node, the $f_i$ is evaluated by the number of CCMs involved in the path, the number of crane motions, and the scaling factor ($\lambda_1$) which is used as input to improve current generation in next generation. Otherwise, the distance from the landing node to the end node is measured and used to calculate the fitness value of the path in current generation. Lastly, the constraints of the crane's permissible range and safety factors are evaluated. If the CCMs of the path are not located in the permissible range of crane operations and the safety factor of the path is more than 85%, the scale factor ($\lambda_2$) is used to subtract it from the overall $f_i$. Based on the experiments by authors, $M_m$, $C_m$, $\lambda_1$, and $\lambda_2$ are determined by 25, 500, 1000, and 20, respectively.

### 3.5.3.2 Selection

After evaluating the fitness of all the paths in the population, the next generation to identify the optimal crane lift path is reproduced by three procedures which are selection, crossover, and

mutation. In the selection, the paths, which have high $f_i$ in previous generation, are selected by the percentage of the best individuals ($P_{best}$) which guarantee the evolution of the results by generations. Selected individuals become parents to generate the children individuals for the next generation by using crossover and mutation.

### 3.5.3.3 Crossover and Mutation

Selected individuals from selection process are used to reproduce a set of new population for the next generation by using two genetic operators, which are crossover and mutation. The crossover rate ($R_c$) enables the lift paths to evolve towards a local optimal solution and the mutation rate ($R_m$) prevents the lift paths not to be stuck in one search area. The $R_c$ is generally a high value between 0.8 and 0.95 to generate the better solutions than the lift paths in previous generation [42]. There are a few types of the crossover such as the single point, multi-point, uniform, and arithmetic method. The multi-point crossover method, which alters some CCMs at the multiple crossing points among the selected lift paths, is adopted in this thesis as described in Fig. 17. In this respect, the crossover is to produce the different characteristics (i.e., CCMs) of the crane lift paths in the next generation which inherits some characteristics of the crane lift paths selected in previous generation.

(a) Crossover point in parent individuals

(b) Generated child individual
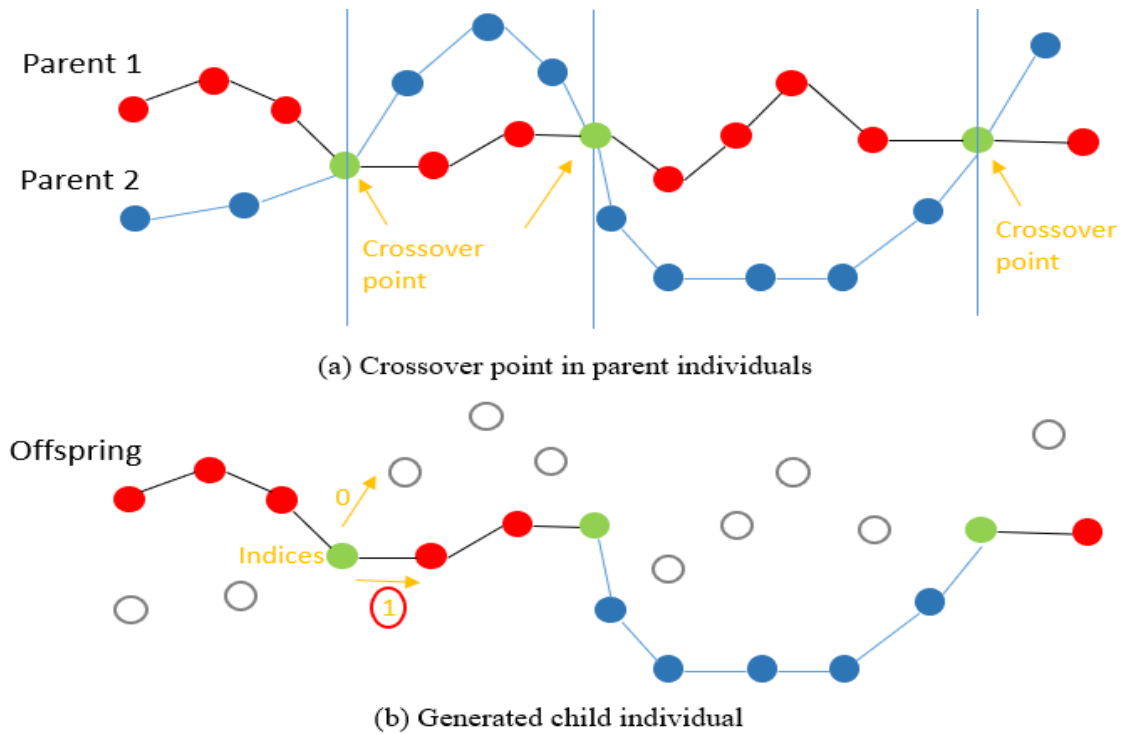
**Figure 17.** Multi-point Crossover

Due to this feature of the crossover, GA can have difficulty to identify the optimal crane lift path by evolving the CCMs of the crane lift paths since the paths may tend to be placed in confinement. To overcome this limitation, a mutation process is required to maintain the diversity of the crane lift paths during the evolution by mutating CCMs randomly and replacing them in the lift paths of succeeding generation. In this respect, the $R_m$ should be a low value between 0.005 and 0.5 since the high value of the $R_m$ leads to pure random searches which make GA slow down the evolution [43].

### 3.5.3.4 Termination

The reproduction process for new generations is repeated until it reaches the number of generation (G) set by users and identifies the optimal lift path which has the highest fitness score. Based on the experiments by authors, $P_{best}$, $R_c$, and $R_m$ are defined by 50%, 0.8, and 0.05, respectively. Furthermore, the initial population in the generation is 50 in this thesis.

41

## 3.6   3D visualization-based mathematical algorithm (3DMVA)

Chapter 2 explains the detail of 3D visualization-based mathematical algorithm (3DMVA). In the Chapter 4. Case study, the results of 3DMVA will be compared with results of other algorithms based on the same project information to identify the advantages and disadvantages of each algorithm.

## 3.7   Comparison Criteria

Previous comparisons of the lift planning algorithms for mobile crane operation mainly focused on the computation time, travelling distance and the number of motions as the comparison criteria [4, 10–14]. These criteria helped to analyze which algorithm provides better performance in terms of the computation costs and less motions during the crane operations. However, it is necessary to improve these criteria, called as the measurement metric in this thesis, in order to evaluate and compare characteristics of algorithms to address the lack of information described in introduction section. In this respect, this thesis introduces five criteria:

1)   The computation time, also called as computation time, which is total time to search for an optimal lifting path.

2)   The travel distance of the lifted object computed by the sum of distances from the start node and to end node on the lifting path identified by algorithms.

3)   The number of crane motions consisting of swing, luffing, and hoisting operations since the changes of crane motions affect the crane operation time in practice.

4)   The expected cycle time of the crane operation for the lifted object corresponding to the practical perspective view considering safety factor, speed of each operations, and the penalty matrix.

5) The success rate which shows the probability to find the solution on different difficulties of site layouts.

At this junction, it should be noted that RRT and GA require to run multiple times to obtain the optimal crane lift paths of lifted objects due to the nature of randomness. Therefore, RRT and GA's success rate is a percentage of pass/fail of the multiple iterations but A * and 3DVMA represent pass/fail of one single iteration.

# Chapter 4:     CASE STUDY

## 4.1   General Information

The case study is implemented using a real industrial project located in Alberta, Canada, which includes 168 modules lifted by crawler cranes mounted with superlift with 660 ton and the boom length is 275 ft. Since the case study has a large number of modules which are lifted on the various site layouts, this thesis selects four modules to facilitate the comparison of the algorithms based on the different types of site layouts in terms of the elevation levels of installing the lifted objects, the lifting sequences scheduled, the number of obstacles on the crane working radius, linear distances between pick points (PPs) and set points (SPs) of the lifted objects, and total CCM differences between the CCM at pick points (PPs) and set points (SPs) of the lifted objects. In terms of total CCM difference, for instance, it is 30 when CCMs at the SP and PP for a module is (5, 5, 5) and (15, 15, 15), respectively. Fig. 18 shows site layouts and the various lift conditions of the selected modules. It is noted that the number of obstacles for the lifted modules are affected by the scheduled sequence and the crane working radius. For example, in the case of module ID 21, the complexity of path planning is relatively low because the elevation level to install the lifted module is the ground floor, the linear distance between the PP and SP is 93.4 ft, and the CCM difference between the PP and SP is 69, which is smaller than others in the lifted modules. Also, there are only three applicable obstacles in the crane working radius among the obstacles with the lower sequence as illustrated in Fig. 19(a).

ID 98
Elevation: 3rd floor
Sequence: 82
Obstacles*: 25
CCM difference: 101

ID 56
Elevation: 1st floor
Sequence: 45
Obstacles*: 12
CCM difference: 104

Pick Position (PP)
Set Position (SP)
Obstacles
Crane Position (CP)

106.73ft
**

103.87ft

ID 32
Elevation: 2nd floor
Sequence: 19
Obstacles*: 3
CCM difference: 127

118.25ft

ID 21
Elevation: 1st floor
Sequence: 32
Obstacles*: 3
CCM difference: 69

93.4ft

*Obstacles indicates the number of relevant obstacles in the crane working radius that were installed before the lifted module ID sequence.
**This is the linear distance between PP and SP.

**Figure 18.** Various lift conditions for four selected modules

Once the site layout is built based on the lifting schedule, A*, RRT, GA, and 3DVMA are implemented to find out the crane lift paths of the selected module and the results are compared by measurement metric. It should be noted that the module 21 is used to describe how these algorithms are applied in the case study.

## 4.2 Case Study Example: Module 21

As shown in Fig. 18, the elevation level is the first floor, sequence of installation is 32, applicable obstacles are three, and CCM difference is 69. Since the sequence of installation of module 21 is 32, 31 modules are installed previously, and these preinstalled modules will behave as the obstacles for module 21. However, only three of those are applicable obstacles that algorithms will consider since those are placed in the crane working radius. In this way, algorithms can avoid unnecessary calculation to provide the results more efficiently.

Before implementing the algorithms, the permissible range of crane motions is defined using the crane specifications and calculations. Based on the crane capacity chart given by the manufacture, the minimum and maximum luffing angles are 28° and 82°, respectively. Since there is no obstacle in the range of the superstructure swing, the permissible range of the superstructure rotation is from 0° to 360°. The length, width and height of module 21 are 24ft, 83ft and 24ft, respectively. The allowable clearances between the boom, existing obstacles and lifted object are defined as 2.5 ft. Lastly, as shown in Fig. 19(b), minimum and maximum lift heights are 25 ft and 246 ft. The dimensions of the existing obstacles, which are modules already installed before lifting the module 21, are identified from the database and applied into the algorithms.
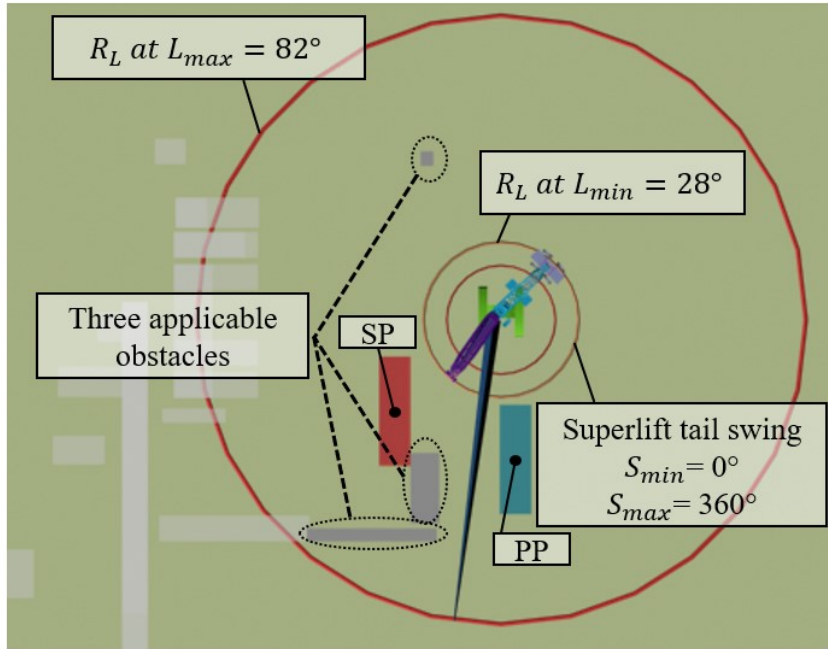
(a) Swing/Luffing ranges and applicable obstacles
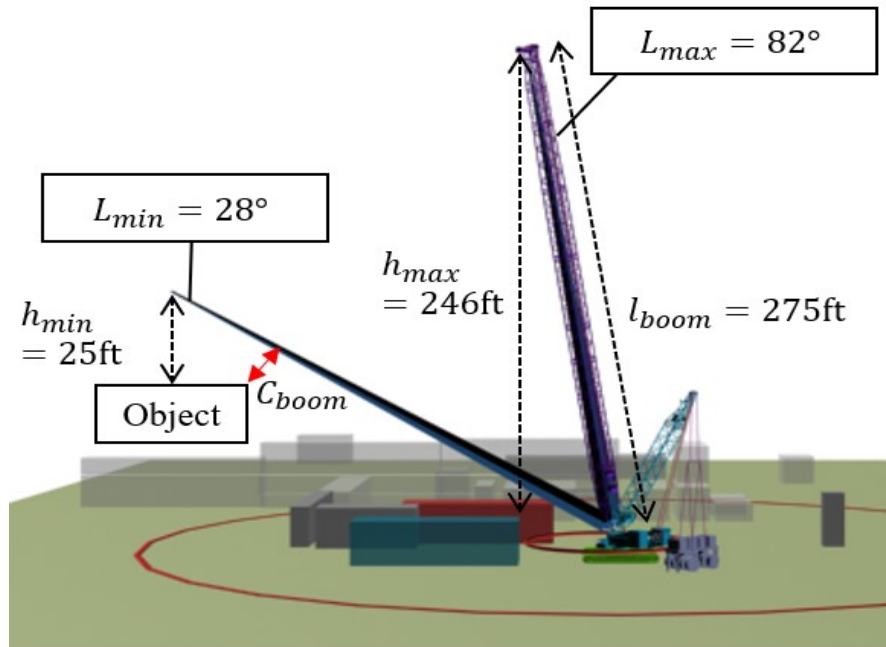


(b) Hoisting ranges

**Figure 19.** Crane permissible range and applicable obstacles in module 21

To calculate the expecting cycle time of a crane lift path, 0.7 rpm for swing and luffing speeds and 171 ft/minute for hoisting speed are used in all of algorithms. Once the project and crane information are defined, optimal crane lift paths are designed by four algorithms.

As an example, Table 4-1 shows the raw result of A* algorithm in the python environment to generate lift path for module 21. It shows the part of lift path generated by A* algorithm. Each row reflects a unit resolution step of either swing, luffing, or hoisting depend on the logic of the algorithm. It also shows the corresponding coordinates of the lifted object, distance that is moved from the previous position, radius, capacity, safety factor, speed, and the operation time.

Table 4-1 Raw result of A* algorithm for module 21 lift planning

|  | S | L | H | x | y | z | Distance | Radius | Capacity | Safety Factor (%) | Speed (ft/min) | Operation Time (s) |
|---|---|---|---|---|---|---|---|---|---|---|---|---|
| 0 | -82 | 72 | 260 | 11.0 | -85.0 | 1.0 | 25.0 | 85.7 | 522500 | 65.2 | 58.0 | 25.9 |
| 1 | -82 | 72 | 235 | 11.0 | -85.0 | 26.0 | 10.5 | 85.7 | 522500 | 65.2 | 60.0 | 1.0 |
| 2 | -82 | 72 | 234 | 11.8 | -84.2 | 15.5 | 1.0 | 85.0 | 546700 | 62.3 | 60.0 | 1.0 |
| 3 | -82 | 72 | 233 | 11.8 | -84.2 | 16.5 | 1.0 | 85.0 | 546700 | 62.3 | 60.0 | 1.0 |
| 4 | -82 | 72 | 232 | 11.8 | -84.2 | 17.5 | 1.0 | 85.0 | 546700 | 62.3 | 60.0 | 1.0 |
| 5 | -82 | 72 | 231 | 11.8 | -84.2 | 18.5 | 1.0 | 85.0 | 546700 | 62.3 | 60.0 | 1.0 |
| 6 | -82 | 72 | 230 | 11.8 | -84.2 | 19.5 | 1.0 | 85.0 | 546700 | 62.3 | 60.0 | 1.0 |
| 7 | -82 | 72 | 229 | 11.8 | -84.2 | 20.5 | 1.0 | 85.0 | 546700 | 62.3 | 60.0 | 1.0 |
| 8 | -82 | 72 | 228 | 11.8 | -84.2 | 21.5 | 1.0 | 85.0 | 546700 | 62.3 | 60.0 | 1.0 |
| 9 | -82 | 72 | 227 | 11.8 | -84.2 | 22.5 | 1.0 | 85.0 | 546700 | 62.3 | 60.0 | 1.0 |
| 10 | -82 | 72 | 226 | 11.8 | -84.2 | 23.5 | 1.0 | 85.0 | 546700 | 62.3 | 60.0 | 1.0 |
| 11 | -82 | 72 | 225 | 11.8 | -84.2 | 24.5 | 1.0 | 85.0 | 546700 | 62.3 | 60.0 | 1.0 |
| 12 | -82 | 72 | 224 | 11.8 | -84.2 | 25.5 | 1.0 | 85.0 | 546700 | 62.3 | 60.0 | 1.0 |
| 13 | -82 | 72 | 223 | 11.8 | -84.2 | 26.5 | 1.0 | 85.0 | 546700 | 62.3 | 60.0 | 1.0 |
| 14 | -82 | 72 | 222 | 11.8 | -84.2 | 27.5 | 1.0 | 85.0 | 546700 | 62.3 | 60.0 | 1.0 |
| 15 | -82 | 72 | 221 | 11.8 | -84.2 | 28.5 | 1.0 | 85.0 | 546700 | 62.3 | 60.0 | 1.0 |
| 16 | -82 | 72 | 220 | 11.8 | -84.2 | 29.5 | 1.0 | 85.0 | 546700 | 62.3 | 60.0 | 1.0 |
| 17 | | | | | | | 1.0 | 85.0 | 546700 | 62.3 | 60.0 | 1.0 |

* S: Swing, L: Luffing, H: Hoisting

To compare the results, it is required to extract the crane motions from this raw result by grouping the consecutive motions. In this respect, Table 4-2 shows the aggregated result from the

raw result. As it shows, the first motion is hosting that moved from 260ft to 214ft. It moved 46 ft, and the time penalty is 1 minute to change to the next motion, which is swing, according to the penalty matrix as shown in Fig. 9. To operate this crane motion, the expected operation time is 46.87 seconds. Once all the crane motions are identified, the sum of time penalty and operation time will be the total expected cycle time.

Table 4-2 Aggregated result of A* algorithm for module 21 lift planning

|  | Motion | Start | End | Difference | Time Penalty (min) | Distance (ft) | Operation Time (s) |
|---|---|---|---|---|---|---|---|
| 0 | Hoisting | 260 ft | 214 ft | 46 | 1 | 46 | 46.87 |
| 1 | Swing | -82 ° | -139° | 57 | 0.75 | 84.54 | 38.70 |
| 2 | Luffing | 72 ° | 67 ° | 5 | 0.5 | 24.00 | 3.88 |
| 3 | Hoisting | 214 ft | 239 ft | 25 | 0 | 25.00 | 31.74 |

Each crane lift path results are generated through the same process. Table 4-3 shows the results of A* and RRT for module 21. As shown in Table 4-3, a total of 4 crane motions are required to deliver the module 21 from the pick point to the set point in A*. The processing time to find the path was 5,085 seconds, the total travelling distance of the module was 179.54 ft, and the total crane operation time (cycle time) was 4.27 minutes.

To design optimal crane lift paths using RRT successfully, expanding the tree from the initial node is determined by two approaches which are: *(i)* to measure the distance from neighboring nodes of the selected node to the set point; and *(ii)* to calculate the different CCM between CCMs of neighboring nodes of the selected node and the CCM at the set point. Each approach was iterated to get an average outcome over a set of 10 iterations to determine the appropriate method that leads to result optimal crane lift paths. In this respect, the final result of each approach in RRT is represented as decimal numbers which are the average results of 10 iterations. As a result, expanding the trees by the distance approach provides the better crane lift path in all aspects of measurement metric than results using the CCM approach in modules 21 case.

At this junction, the procedures to identify the best approach for other modules are also implemented since each lifted module has various lifting conditions such as site layouts, distances from pick points, CCM differences to set points and installation levels. In addition, the number of iterations is determined based on the experiments implemented by authors.

Table 4-3 Results of A* and RRT for Module 21

| | | Iteration | Computation Time (s) | Travel Distance (ft) | # of crane motions | | | | Cycle time (min) | Success rate (%) |
|---|---|---|---|---|---|---|---|---|---|---|
| | | | | | S | L | H | Total | | |
| A* | | 1 | 5085.3 | 179.5 | 1 | 1 | 2 | 4 | 4.3 | 100 |
| RRT | Distance | 10 | 37.1 | 217.0 | 18.0 | 3.1 | 19.4 | 40.5 | 32.8 | 100 |
| | CCM | 10 | 56.2 | 262.6 | 27.3 | 7.2 | 28.1 | 62.6 | 49.6 | 100 |

*S: Swing, L: Luffing, H: Hoisting

GA was tested with various numbers of generations which are 20, 50, 100, 200, 500, 1000, 2000, 4000, and 8000 in order to identify the evolution of results by increasing the generation that leads to find the optimal crane path. Each generation was iterated 10 times to have the reliable and optimal crane lift paths. Table 4-4 represents the results which are acquired based on different generations in GA for module 21. When the number of generations in GA set as 100, the average computation time was 36.8 seconds, the average travel distance was 199.7 ft, the average number of motions was 22.8, and the average expecting crane operation time was 18.0 minutes. Also, among 10 iterations, the success rate to find the optimal crane lift path was 40%. By increasing the number of generations, the number of total motions and expecting cycle time of crane operation tend to decrease but the computation time and the success rate increase. However, the travel distances are not affected by the number of generations. Although GA is designed to find optimal crane lift paths with the least number of crane motions and expecting cycle times of crane operations when the number of generations is increased, the increase of the computation time

cannot be ignored to select an algorithm of crane lift paths since the designing times and costs for crane lift paths become large and expensive in heavy industrial construction projects which involve a large number of modules. Therefore, this thesis selects a number of generations that reaches 100 % of success rate for the first time. In this respect, 500 generation is selected for module 21 which provides 100 % of success rate for the first time. This GA generation tests for other modules are implemented and the number of generations for each of other modules are various due to different site layouts and constraints (e.g., number of obstacles).

Table 4-4 Results of GA with generations in Module 21

| Generation | Computation Time (s) | Travel Distance (ft) | # of crane motions | | | | Cycle Time (min) | Success Rate (%) |
|---|---|---|---|---|---|---|---|---|
| | | | S | L | H | Total | | |
| 20 | 5.5 | 180.2 | 8.7 | 5.9 | 8.6 | 23.2 | 17.0 | 0 |
| 50 | 18.3 | 200.1 | 9.7 | 6.2 | 9.2 | 25.1 | 19.0 | 10 |
| 100 | 36.8 | 199.7 | 9.4 | 5.1 | 8.3 | 22.8 | 18.0 | 40 |
| 200 | 93.2 | 211.4 | 8.8 | 4.8 | 8.2 | 21.8 | 17.2 | 70 |
| 500 | 262.3 | 203.9 | 7.5 | 3.7 | 7.4 | 18.6 | 14.8 | 100 |
| 1000 | 606.4 | 194.8 | 5.3 | 3.2 | 5.6 | 14.1 | 12.0 | 100 |
| 2000 | 1143.7 | 208.7 | 4.3 | 2.7 | 4.3 | 11.3 | 10.2 | 100 |
| 4000 | 2013.1 | 216.0 | 3.3 | 2.0 | 5.0 | 10.3 | 9.2 | 100 |
| 8000 | 4870.9 | 201.6 | 4.0 | 2.3 | 4.0 | 10.3 | 9.5 | 100 |

Since 3DVMA [28] uses 3D visualization-based mathematical models, it either designs only one single crane lift path for each of the lifted objects or fails to provide a crane lift path, which means it doesn't require the iteration. In this respect, 3DVMA succeeds to design the crane lift path for module 21 which contains 321 seconds for computation time, 321 ft for travel distance, 8 crane motions and approximately 5 minutes for expecting cycle time of crane operation.

Once the crane lift paths are designed by algorithms and evaluated by the measurement metrics, the CCMs of the crane lift paths are visualized in 3D environment for validation in terms of collision-free and further analysis such as patterns of the crane lift paths which can help to determine if the crane lift paths designed by algorithms can not only satisfy the mobility of mobile crane fully but also be accepted by industry practically. In this respect, as shown in Fig. 21, A* and 3DVMA generate a similar trend which consists of a simple and practical mobility of the mobile crane operation that has less numbers of mobile crane motions. However, RRT and GA tend to have a greater number of mobile crane motions comparing to the results of A* and 3DVMA. This large number of crane motion changes can lead to the following results: (*i*) to increase the expecting cycle times of crane operation; (*ii*) to increase the collision risks during the crane motion changes which are not preferred and acceptable crane lift paths in practice; and (*iii*) a zig-zag pattern (e.g., vertically and horizontally up and down) resulting the unpractical crane lift even though the path satisfies the requirements of the natural mobility of mobile cranes.
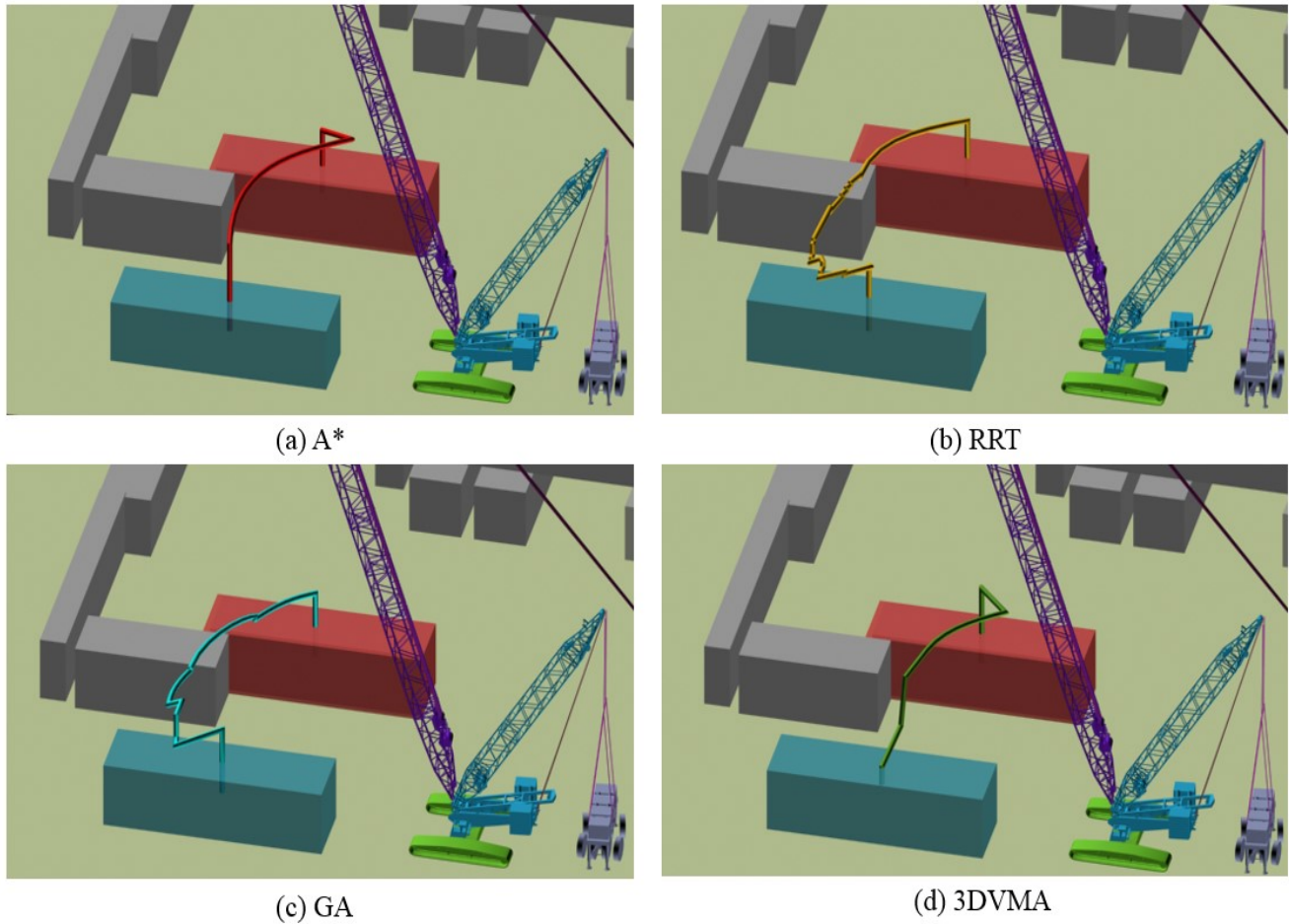
**Figure 20.** 3D visualization of crane lift paths for module 21

## 4.3   Combined Results

Based on the same procedures used for module 21, crane lift paths for other modules have been designed by algorithms and evaluated by the measurement metric. As a result, Table 4-5 represents the results of evaluation using measurement metric for four selected modules, which are module 21, 32, 56, and 98.

According to the site and lift path conditions such as the number of obstacles on the work radius, elevation level for installation, distance between the PP and the SP and CCM difference between the PP and SP, each algorithm generates different characteristics of the optimal crane lift paths. A* search plans the optimal crane lift paths for all of modules which involve minimum

expected cycle time of the crane operations due to a smaller number of crane motions than ones in other algorithms. However, as shown in Fig. 22(a) and (b), the computation times to design the optimal crane lift paths are tremendously increased when both the distances and CCM difference between the SPs and PPs are increased. This trend is caused by: (*i*) large-scale construction sites which lead to generate the huge search space including massive coordinates evaluated by A* search; and (*ii*) the characteristic of A* search which keeps all the previous CCMs to identify the optimal crane lift path using heuristic function until reaching to the goal node. As an example of the first cause, in the case of module 32, total 129,527 CCMs were evaluated during the computation time, 212705.1 seconds; whereas module 21 tested a total of 8,895 CCMs within 5085.3 seconds.

Comparing to other algorithms, RRT provides the result in the shortest computation time regardless the complexity of the site layouts since it rapidly explores the searching areas without concerning neighborhood nodes unlike A* search. In a practical view, the crane lift paths identified by RRT may not be suitable since the expecting cycle times of crane operations affected by the number of crane motions shown in Fig. 22(c) are the highest among other algorithms. The reason of this feature is that RRT is based on randomness and it has a nature of generating zig-zag patterns to search for the crane lift paths. Although RRT succeeds to find the feasible paths in the shortest computation time, it does not have an optimization function comparing to the heuristic search in A* and the evolution process in GA in order to not only reduce the number of crane motions but also design practical motions of mobile crane operation (e.g., prevention of zig-zag motions).

As shown in Fig. 22(b), the computation times of GA are influenced by the CCM difference which represents the level of site complexity. In this respect, the increase of the CCM difference can result many failures in the phase of reproducing initial populations which is required to provide

the sources to run the next generation for the feasible crane lift paths. When these paths are designed successfully, the paths are evolved in the way of shortening the number of motions as defined in the fitness evaluation. Comparing to the results of other algorithms based on the practical motions of the mobile crane lift and number of crane motions, GA provides better practical lift paths than RRT, with less computation time than A*. One of advantages in GA is flexible application in various sizes and complexity of sites based on the input changes such as generations, populations, mutation rate, and crossover rate. For example, the number of generations to compare to other algorithms in this thesis is the generation that obtains the success rate of 100% for the first. To optimize smooth lift paths such as ones in A* and 3DVMA, the number of generations can be increased but this requires more process times. Therefore, GA results can be flexible depend on the focus of the outcomes.

Based on the view of results in the measurement metrics, 3DVMA requires less process time than other algorithms except RRT to design crane lift paths which represent smooth and practical crane motions with small number of crane motion changes leading to the shorter expected cycle times of crane operations than other algorithms except A*. However, this algorithm may not have flexibility to other types of projects which may have different lift design constraints due to the following reasons: (*i*) 3DVMA is not fully validated yet in other types of projects but others done by previous research; and (*ii*) it does not have randomness search functions with/without evolutions; and (*iii*) the crane lift paths designed by 3DVMA may not be optimal paths since it follows the practical and preferred sequences of crane motions defined by the users.

Table 4-5 Results of algorithms

| Module | Algorithm | Process Time (s) | Travel Distance (ft) | # of crane motions | | | | Cycle time (min) | Success Rate (%) |
|--------|-----------|------------------|---------------------|------|------|------|-------|------------------|------------------|
| | | | | S | L | H | Total | | |
| **21** | A* | 5085.3 | 189.1 | 1.0 | 1.0 | 2.0 | 4.0 | 4.3 | Pass |
| | RRT (distance) | 37.1 | 217.0 | 18.0 | 3.1 | 19.4 | 40.5 | 32.8 | 100 |
| | GA (500) | 262.3 | 203.9 | 7.5 | 3.7 | 7.4 | 18.6 | 14.8 | 100 |
| | 3DVMA | 321.0 | 158.7 | 3.0 | 2.0 | 3.0 | 8.0 | 5.0 | Pass |
| **32** | A* | 212705.1 | 257.5 | 1.0 | 1.0 | 2.0 | 4.0 | 4.6 | Pass |
| | RRT (distance) | 6.2 | 384.1 | 33.9 | 23.5 | 35.2 | 92.6 | 74.0 | 100 |
| | GA (4000) | 9470.0 | 290.2 | 6.3 | 5.0 | 7.7 | 19.0 | 17.0 | 100 |
| | 3DVMA | 200.0 | 156.8 | 3.0 | 1.0 | 4.0 | 8.0 | 5.8 | Pass |
| **56** | A* | 24526.8 | 201.5 | 4.0 | 2.0 | 7.0 | 13.0 | 10.0 | Pass |
| | RRT (distance) | 28.8 | 228.1 | 15.9 | 11.0 | 14.9 | 41.8 | 31.5 | 100 |
| | GA (2000) | 5132.1 | 225.0 | 6.0 | 4.3 | 5.7 | 16.0 | 13.3 | 100 |
| | 3DVMA | 335.0 | 525.4 | 4.0 | 1.0 | 4.0 | 9.0 | 10.6 | Pass |
| **98** | A* | 25146.2 | 208.1 | 1.0 | 1.0 | 3.0 | 5.0 | 6.4 | Pass |
| | RRT (distance) | 11.8 | 204.5 | 22.8 | 2.2 | 23.8 | 48.8 | 38.9 | 100 |
| | GA (1000) | 2116.6 | 229.7 | 7.0 | 2.1 | 7.4 | 16.5 | 15.1 | 100 |
| | 3DVMA | 661.0 | 157.6 | 2.0 | 1.0 | 4.0 | 7.0 | 7.0 | Pass |
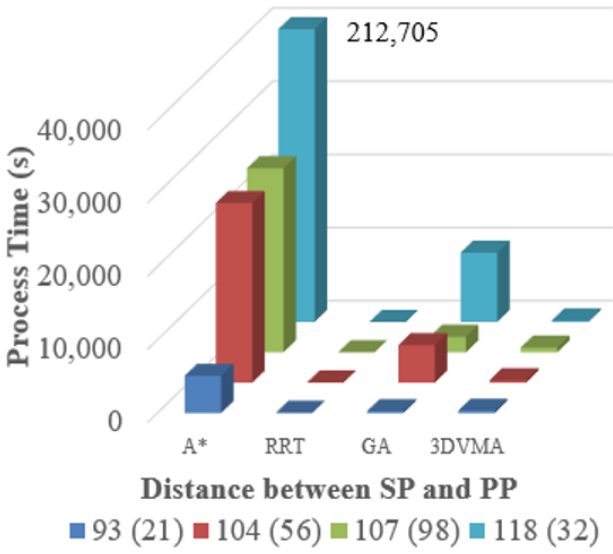
(a)
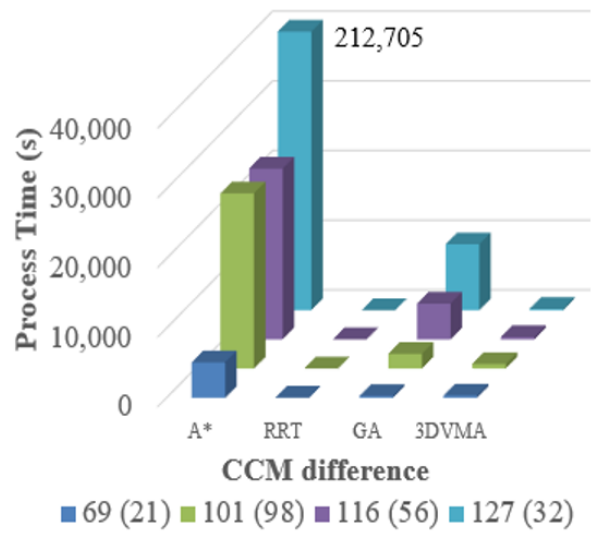


(b)
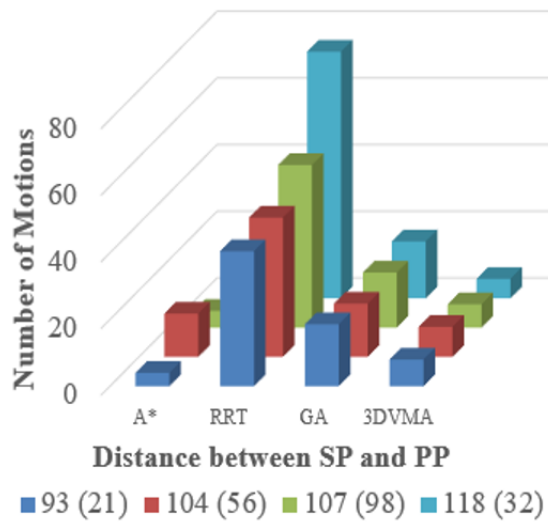


(c)

**Figure 21.** 3D visualization of crane lift paths for module 21

# Chapter 5:    CONCLUSIONS AND FUTURE WORK

## 5.1  Conclusions

Due to a numerous number of modules lifted mainly by mobile cranes in heavy industrial projects, the lift path planning has been highly attention to design the efficient and safe mobile crane operations which influence to improve productivity and safety. This lift path planning analysis can be done mainly in not only the planning phase of the project, but also in the construction phase. Since heavy industrial projects involve a large number of lift operations, this lift analysis helps to predict the total required time for the lift operation used for the equipment management and scheduling in the planning phase. In the construction phase, the lift analysis can be done for any changes on site, which is more efficient and faster than manual analysis by the lift engineer. Although previous research introduces algorithms which are applied to plan the optimal crane lift paths leading to support the project schedule before construction, there is no comprehensive comparison study yet to identify the best algorithm based on considering the features of the heavy industrial projects such as dynamic site layout changes and a large number of modules (generally 200-300 modules to be lifted per project) which should satisfy the following requirements: *(i)* fast computation time without design errors; *(ii)* collision-free lifts; *(iii)* less expected cycle times of crane operations; and *(iv)* applying practical mobility of mobile crane lifts. Furthermore, the lack of this study may be one of main barriers to facilitate to apply the proposed optimal algorithms into the crane lift path planning in practice in accordance with the features of their projects. To address this challenge, this thesis implements the comprehensive comparison study using A* search, RRT, GA, and 3DVMA in mobile crane path optimization problem with the measurement metrics.

Based on the results of the case study, all algorithms do not have any collision issues in the crane lift paths designed by this study. In other words, all algorithms generate collision-free crane lift paths without matters issued by the features of the heavy industrial projects (e.g., congested and dynamic site layouts). In terms of nature mobility of the mobile crane, RRT is not suitable in heavy industrial projects since it tends to produce the zig-zag pattern leading to produce the largest number of crane motions and highest expected cycle times. Due to this feature, the crane lifts designed by RRT considers as unsafe, impractical and inefficient lifts even though the shortest computation times are achieved. GA plans acceptable crane lifts without matters issued by the site constraints such as number of obstacles and linear distances. Since the number of generations in GA is defined as first generation that obtains the success rate of 100% in this thesis, the crane lift paths resulted by GA can be improved by adjusting parameters such as number of generations, crossover rate, and mutual rate for each lift. Due to the difficulty of finding the proper parameters and their relationship to implement into the fitness evaluation, GA may not be the best algorithm for numerous numbers of lifts in the heavy industrial projects. As a result, the best results are designed by A* and 3DVMA due to smaller number of motions and smooth trajectories of crane lifts than ones from the other algorithms. At this junction, it should be noted that the practitioners consider that crane lifts are potentially high risk when the number of motions is large. In this respect, A* designs more safe crane lifts than 3DVMA in most of cases except module ID 56. However, A* requires large computation times which are maximum 3545 minutes and minimum 84 minutes to design one single crane lift paths.

Table 5-1 Heavy industrial project characteristics & algorithm suitability

| | Large # of Modules | Flexibility | Practicality | Dynamic Site Layout | Mobile Crane Configuration |
|---|---|---|---|---|---|
| **A\*** | X | X | O | O | O |
| **RRT** | O | O | X | O | O |
| **GA** | Δ | O | Δ | O | O |
| **3DMVA** | O | X | O | O | O |

\* Δ represents undefined/unknown.

Table 5-1 shows the characteristics of heavy industrial project and the suitability of algorithms. Regarding to the large number of modules, A* is not beneficial because of its tremendous computation time, and GA is undefined since the results may vary depending on the number of generations. Also, A* and 3DMVA are lack of flexibility since those are deterministic algorithm, which means that it only generates one possible solution for the problem. In terms of practicality, RRT is not beneficial because of its unfeasible solution. Therefore, A* is not fitted in heavy industrial projects but may be the best model when the computation time can be significantly reduced and there is no need for the extra solutions. Based on considering all requirements described above, 3DVMA is a competent crane lift path planning method for heavy industrial projects. However, as shown in the case of module ID 56, it has a limitation which is the lack of an evolution/search function to optimize crane lift paths in terms of the travel distance affecting the expected cycle times of the crane lifts even though it produces a smaller number of motions than A*'s one. In this respect, this algorithm requires additional improvement by integrating with the strengths of other optimization algorithms such as evolution functions.

## 5.2  Contributions

The main contribution of the current research is described below:

1) Various algorithms for the lift path planning of the mobile crane were implemented in the heavy industrial project with the consideration of the dynamic site layout and realistic crane mobility.

2) The results of the lift path planning in each algorithm were compared comprehensively based on the multi-measurement matrix and site constraints, which represent the advantages and disadvantages of each algorithm more accusatively than previous studies.

5) The outcome of this research suggested the direction of lift path planning algorithm for mobile crane that integrates the advantages of compared algorithms for the future work to accomplish the automation of the construction industry.

## 5.3  Limitations and Future Work

In the current methodology, the algorithms are developed with the limited operation type, which is PFP, with 3 active DOFs. Future works could implement all kind of collision types for the collision detection and the PWO operation with more DOFs to fully simulate the path planning result that reflects more realistic environment.

For the algorithm based on the randomness such as RRT and GA, several inputs such as sample rate of RRT and crossover rate, mutation rate, population, initial size of population, and generation of GA are adopted from the previous research or experiments in the current thesis, which can be customized in each module case to draw the best result.

Since current study only considered algorithms that previously applied in the lift path planning for the mobile crane operation, other widely used algorithms for the path planning such as anti colony optimization algorithm could be implemented and compared with the current results for the future works.

The combined parallel hybrid algorithm with the advantages of three algorithms can be suggested in the future works for the mobile crane path planning. For instance, with evaluating the complexity of the path finding problem automatically, A* search can be executed for the low complexity problems while hybrid algorithms with RRT and GA is executed for the high complexity problems. Since RRT is beneficial to find solutions in short time, the results of RRT can be used to generate the initial population of the GA that could reduce computation time of GA significantly while improving the quality of the result.

# Reference

[1] S. H. Han, S. Hasan, A. Bouferguène, M. Al-Hussein, and J. Kosa, "Utilization of 3D Visualization of Mobile Crane Operations for Modular Construction On-Site Assembly," *Journal of Management in Engineering*, vol. 31, no. 5, p. 04014080, Sep. 2015, doi: 10.1061/(ASCE)ME.1943-5479.0000317.

[2] J. Olearczyk, M. Al-Hussein, and A. Bouferguène, "Evolution of the crane selection and on-site utilization process for modular construction multilifts," *Automation in Construction*, vol. 43, pp. 59–72, Jul. 2014, doi: 10.1016/j.autcon.2014.03.015.

[3] "eLCOSH : Understanding Crane Accident Failures: A report on the causes of death in crane-related accidents," *http://www.elcosh.org/document/2053/d001029/Understanding+Crane+Accident+Failures%3A+A+report+on+the+causes+of+death+in+crane-related+accidents.html*, 2010. [Online]. Available: http://www.elcosh.org/document/2053/d001029/Understanding+Crane+Accident+Failures%3A+A+report+on+the+causes+of+death+in+crane-related+accidents.html. [Accessed: 29-Mar-2019].

[4] P. Cai, Y. Cai, I. Chandrasekaran, and J. Zheng, "Parallel genetic algorithm based automatic path planning for crane lifting in complex environments," *Automation in Construction*, vol. 62, pp. 133–147, Feb. 2016, doi: 10.1016/j.autcon.2015.09.007.

[5] Z. Lei, S. Han, A. Bouferguène, H. Taghaddos, U. Hermann, and M. Al-Hussein, "Algorithm for Mobile Crane Walking Path Planning in Congested Industrial Plants," *Journal of Construction Engineering and Management*, vol. 141, no. 2, p. 05014016, Feb. 2015, doi: 10.1061/(ASCE)CO.1943-7862.0000929.

[6] Lin Kuo-Liang and Haas Carl T., "An Interactive Planning Environment for Critical Operations," *Journal of Construction Engineering and Management*, vol. 122, no. 3, pp. 212–222, Sep. 1996, doi: 10.1061/(ASCE)0733-9364(1996)122:3(212).

[7] Hornaday W. C., Haas C. T., O'Connor J. T., and Wen J., "Computer-Aided Planning for Heavy Lifts," *Journal of Construction Engineering and Management*, vol. 119, no. 3, pp. 498–515, Sep. 1993, doi: 10.1061/(ASCE)0733-9364(1993)119:3(498).

[8] J. Olearczyk, A. Bouferguène, M. Al-Hussein, and U. (Rick) Hermann, "Automating motion trajectory Of crane-lifted loads," *Automation in Construction*, vol. 45, pp. 178–186, Sep. 2014, doi: 10.1016/j.autcon.2014.06.001.

[9] Z. Lei, H. Taghaddos, U. Hermann, and M. Al-Hussein, "A methodology for mobile crane lift path checking in heavy industrial projects," *Automation in Construction*, vol. 31, pp. 41–53, May 2013, doi: 10.1016/j.autcon.2012.11.042.

[10] A. R. Soltani, H. Tawfik, J. Y. Goulermas, and T. Fernando, "Path planning in construction sites: performance evaluation of the Dijkstra, A∗, and GA search algorithms," *Advanced Engineering Informatics*, vol. 16, no. 4, pp. 291–303, Oct. 2002, doi: 10.1016/S1474-0346(03)00018-1.

[11] Pl. Sivakumar, K. Varghese, and N. R. Babu, "Automated Path Planning of Cooperative Crane Lifts Using Heuristic Search," *Journal of Computing in Civil Engineering*, vol. 17, no. 3, p. 197, Jul. 2003.

[12] M. S. A. D. Ali, N. R. Babu, and K. Varghese, "Collision Free Path Planning of Cooperative Crane Manipulators Using Genetic Algorithm," *Journal of Computing in Civil Engineering*, vol. 19, no. 2, pp. 182–193, Apr. 2005, doi: 10.1061/(ASCE)0887-3801(2005)19:2(182).

[13] Y.-C. Chang, W.-H. Hung, and S.-C. Kang, "A fast path planning method for single and dual crane erections," *Automation in Construction*, vol. 22, pp. 468–480, Mar. 2012, doi: 10.1016/j.autcon.2011.11.006.

[14] Y. Lin, D. Wu, X. Wang, X. Wang, and S. Gao, "Lift path planning for a nonholonomic crawler crane," *Automation in Construction*, vol. 44, pp. 12–24, Aug. 2014, doi: 10.1016/j.autcon.2014.03.007.

[15] C. Zhang and A. Hammad, "Improving lifting motion planning and re-planning of cranes with consideration for safety and efficiency," *Advanced Engineering Informatics*, vol. 26, no. 2, pp. 396–410, Apr. 2012, doi: 10.1016/j.aei.2012.01.003.

[16] Yuanshan Lin, Hong Yu, Geng Sun, and Penghui Shi, "Lift Path Planning without Prior Picking/Placing Configurations: Using Crane Location Regions," *Journal of Computing in Civil Engineering*, vol. 30, no. 1, pp. 1–12, Feb. 2016, doi: 10.1061/(ASCE)CP.1943-5487.0000437.

[17] C. Zhang and A. Hammad, "Multiagent Approach for Real-Time Collision Avoidance and Path Replanning for Cranes," *Journal of Computing in Civil Engineering*, vol. 26, no. 6, pp. 782–794, Nov. 2012, doi: 10.1061/(ASCE)CP.1943-5487.0000181.

[18] M. Y. Cheng and J. T. O'Connor, "ArcSite: Enhanced GIS for Construction Site Layout," *Journal of Construction Engineering and Management*, vol. 122, no. 4, pp. 329–336, Dec. 1996, doi: 10.1061/(ASCE)0733-9364(1996)122:4(329).

[19] M. J. Mawdesley, S. H. Al-jibouri, and H. Yang, "Genetic Algorithms for Construction Site Layout in Project Planning," *Journal of Construction Engineering and Management*, vol. 128, no. 5, pp. 418–426, Oct. 2002, doi: 10.1061/(ASCE)0733-9364(2002)128:5(418).

[20] H. M. Sanad, M. A. Ammar, and M. E. Ibrahim, "Optimal Construction Site Layout Considering Safety and Environmental Aspects," *Journal of Construction Engineering and Management*, vol. 134, no. 7, pp. 536–544, Jul. 2008, doi: 10.1061/(ASCE)0733-9364(2008)134:7(536).

[21] J. Xu and Z. Li, "Multi-Objective Dynamic Construction Site Layout Planning in Fuzzy Random Environment," *Automation in Construction*, vol. 27, pp. 155–169, Nov. 2012, doi: 10.1016/j.autcon.2012.05.017.

[22] C. Huang, C. K. Wong, and C. M. Tam, "Optimization of tower crane and material supply locations in a high-rise building site by mixed-integer linear programming," *Automation in Construction*, vol. 20, no. 5, pp. 571–580, Aug. 2011, doi: 10.1016/j.autcon.2010.11.023.

[23] A. S. Hanna and W. B. Lotfallah, "A fuzzy logic approach to the selection of cranes," *Automation in Construction*, vol. 8, no. 5, pp. 597–608, Jun. 1999, doi: 10.1016/S0926-5805(99)00009-6.

[24] M. Al-Hussein, O. Moselhi, and S. Alkass, "An algorithm for mobile crane selection and location on construction sites," *Construction Innovation*, vol. 1, no. 2, pp. 91–105, Jun. 2001, doi: 10.1108/14714170110814532.

[25] Wu Di, Lin Yuanshan, Wang Xin, Wang Xiukun, and Gao Shunde, "Algorithm of Crane Selection for Heavy Lifts," *Journal of Computing in Civil Engineering*, vol. 25, no. 1, pp. 57–65, Jan. 2011, doi: 10.1061/(ASCE)CP.1943-5487.0000065.

[26] Z. Lei, H. Taghaddos, J. Olearczyk, M. Al-Hussein, and U. Hermann, "Automated Method for Checking Crane Paths for Heavy Lifts in Industrial Projects," *Journal of Construction Engineering and Management*, vol. 139, no. 10, p. 04013011, Oct. 2013, doi: 10.1061/(ASCE)CO.1943-7862.0000740.

[27] M. S. A. D. Ali, N. R. Babu, and K. Varghese, "Offline Path Planning of cooperative manipulators using Co-Evolutionary Genetic Algorithm," in *Proceedings of the International Symposium on Automation and Robotics in Construction, 19th (ISARC*, 2002.

[28] S. Han, Z. Lei, A. Bouferguene, M. Al-Hussein, and U. (Rick) Hermann, "3D Visualization-Based Motion Planning of Mobile Crane Operations in Heavy Industrial Projects," *Journal of Computing in Civil Engineering*, vol. 30, no. 1, p. 04014127, Jan. 2016, doi: 10.1061/(ASCE)CP.1943-5487.0000467.

[29] S. Han, A. Bouferguene, M. Al-Hussein, and U. (Rick) Hermann, "3D-Based Crane Evaluation System for Mobile Crane Operation Selection on Modular-Based Heavy Construction Sites," *Journal of Construction Engineering and Management*, vol. 143, no. 9, p. 04017060, Sep. 2017, doi: 10.1061/(ASCE)CO.1943-7862.0001360.

[30] K. Rich, E. K., *Artificial Intelligence*. New York: McGraw-Hill, 1991.

[31] P. E. Hart, N. J. Nilsson, and B. Raphael, "A Formal Basis for the Heuristic Determination of Minimum Cost Paths," *IEEE Transactions on Systems Science and Cybernetics*, vol. 4, no. 2, pp. 100–107, Jul. 1968, doi: 10.1109/TSSC.1968.300136.

[32] E. W. Dijkstra, "A note on two problems in connexion with graphs," *Numerische Mathematik*, vol. 1, no. 1, pp. 269–271, Dec. 1959, doi: 10.1007/BF01386390.

[33] Choset, H., "Robotic Motion Planning: A* and D* Search," 2015. [Online]. Available: http://www.cs.cmu.edu/~motionplanning/lecture/lecture.html. [Accessed: 29-Nov-2018].

[34] S. M. Lavalle, "Rapidly-Exploring Random Trees: A New Tool for Path Planning," 1998.

[35] J. Bruce and M. M. Veloso, "Real-Time Randomized Path Planning for Robot Navigation," in *RoboCup 2002: Robot Soccer World Cup VI*, 2003, pp. 288–295.

[36] S. M. LaValle, J. J. Kuffner, and Jr., *Rapidly-Exploring Random Trees: Progress and Prospects*. 2000.

[37] D. E. Goldberg, *Genetic Algorithms in Search, Optimization and Machine Learning*, 1st ed. Boston, MA, USA: Addison-Wesley Longman Publishing Co., Inc., 1989.

[38] N. Saini, "Review of Selection Methods in Genetic Algorithms," *1*, vol. 6, no. 12, pp. 22261–22263, Dec. 2017.

[39] S. M. Udupa, "Collision detection and avoidance in computer controlled manipulators," PhD Thesis, California Institute of Technology, 1977.

[40] T. Lozano-Pérez and M. A. Wesley, "An Algorithm for Planning Collision-free Paths Among Polyhedral Obstacles," *Commun. ACM*, vol. 22, no. 10, pp. 560–570, Oct. 1979, doi: 10.1145/359156.359164.

[41] H. Choset, "Robotic Motion Planning: Sample-Based Motion Planning," p. 109.

[42] *Grid Computing: The New Frontier of High Performance Computing*, vol. 14. Elsevier Science.

[43] M. Srinivas and L. M. Patnaik, "Adaptive probabilities of crossover and mutation in genetic algorithms," *IEEE Transactions on Systems, Man, and Cybernetics*, vol. 24, no. 4, pp. 656–667, Apr. 1994, doi: 10.1109/21.286385.

# APPENDIX A: Capacity Check

Reference: https://www.barnhartcrane.com/cranecharts/cc-2800_600t_demag.pdf

- Working ranges main boom with superlift
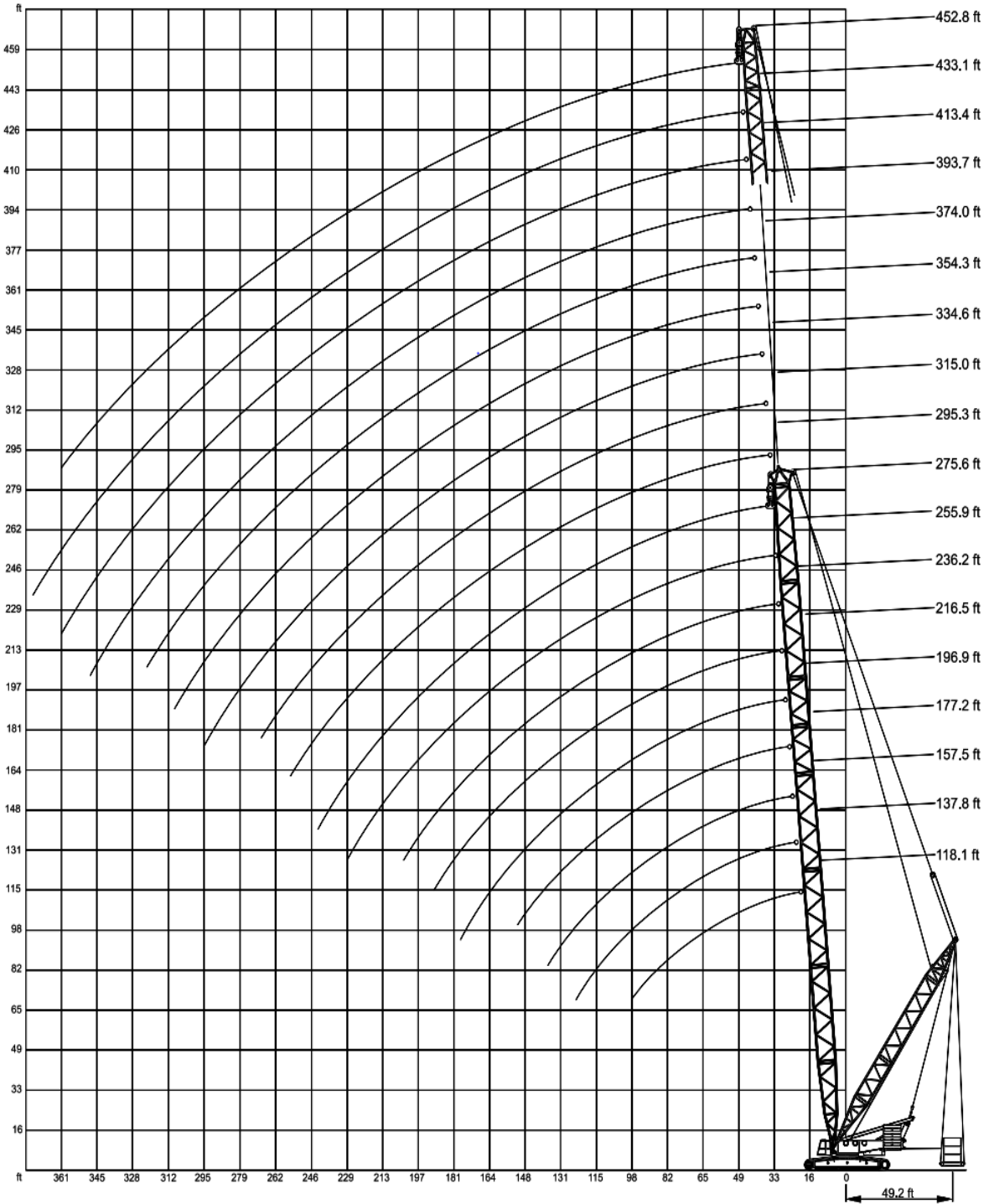
- Lifting Capacity main boom with superlift

# Main boom: 275.6 ft    SL-Radius 49.2 ft

397,000 lb[1)]    27.6 ft    360°

| Radius lb | 0 | 110.2 | 220.5 | 330.7 | 440.9 | 551.2 | 661.4 | 716.5 |
|---|---|---|---|---|---|---|---|---|
| ft | | | | 1,000 lb | | | | |
| 39 | 549.0 | 595.2 | 601.9 | – | – | – | – | 619.5 |
| 46 | 423.3 | 582.0 | 590.8 | 599.7 | – | – | – | 619.5 |
| 52 | 341.7 | 471.8 | 579.8 | 590.8 | 604.1 | – | – | 619.5 |
| 59 | 282.2 | 394.6 | 507.1 | 584.2 | 599.7 | 619.5 | – | 619.5 |
| 65 | 238.1 | 337.3 | 434.3 | 531.3 | 586.4 | 608.5 | – | 608.5 |
| 72 | 205.0 | 291.0 | 379.2 | 465.2 | 551.2 | 588.6 | 588.6 | 588.6 |
| 79 | 178.6 | 255.7 | 332.9 | 412.3 | 489.4 | 568.8 | 568.8 | 568.8 |
| 85 | 156.5 | 227.1 | 297.6 | 368.2 | 438.7 | 509.3 | 546.7 | 546.7 |
| 92 | 136.7 | 202.8 | 266.8 | 332.9 | 396.8 | 460.8 | 522.5 | 522.5 |
| 98 | 121.3 | 180.8 | 242.5 | 302.0 | 361.6 | 421.1 | 480.6 | 491.6 |
| 111 | 97.0 | 149.9 | 200.6 | 253.5 | 304.2 | 357.1 | 407.9 | 421.1 |
| 124 | 77.2 | 123.5 | 169.8 | 216.1 | 262.4 | 306.4 | 352.7 | 366.0 |
| 138 | 61.7 | 105.8 | 145.5 | 187.4 | 227.1 | 269.0 | 308.6 | 321.9 |
| 151 | 48.5 | 88.2 | 125.7 | 163.1 | 200.6 | 235.9 | 273.4 | 286.6 |
| 164 | 39.7 | 75.0 | 110.2 | 143.3 | 176.4 | 211.6 | 244.7 | 255.7 |
| 177 | 30.9 | 63.9 | 97.0 | 127.9 | 158.7 | 189.6 | 220.5 | 231.5 |
| 190 | 24.3 | 55.1 | 83.8 | 114.6 | 143.3 | 172.0 | 200.6 | 211.6 |
| 203 | 17.6 | 46.3 | 75.0 | 103.6 | 130.1 | 156.5 | 183.0 | 191.8 |
| 216 | 13.2 | 39.7 | 66.1 | 92.6 | 116.8 | 143.3 | 167.6 | 169.8 |
| 230 | – | 33.1 | 59.5 | 83.8 | 108.0 | 132.3 | 152.1 | 152.1 |
| 243 | – | 28.7 | 52.9 | 75.0 | 99.2 | 121.3 | 134.5 | 134.5 |

SSL (label beside rows beginning at 98)

For example, in module 21 case, the weight of the module is 313,926 lbs. If current working radius is 95 ft, 98 ft is used in the lifting capacity chart between 92 ft and 98ft because 98ft has smaller gross capacity. Therefore, the gross capacity becomes 421,100lbs. Then, Safety factor is 313,926lbs/421,100lbs x 100% = 74.5 %.

70

# APPENDIX B: Module Information

| | Object ID | 21 | 32 | 56 | 98 |
|---|---|---|---|---|---|
| | Tracking ID | 2068 | 3453 | 5631 | 11834 |
| **Crane Coordinates** | x | 100045 | 99955 | 99665 | 99550 |
| | y | 71625 | 71680 | 71690 | 71500 |
| | z | 1173.74 | 1173.74 | 1173.74 | 1173.74 |
| **Module Pick Coordinates** | x | 100056.4 | 99923 | 99600 | 99474 |
| | y | 71539.59 | 71623 | 71625 | 71560 |
| | z | 1175 | 1175 | 1175 | 1175 |
| **Module Set Coordinates** | x | 99964.4 | 99823.65 | 99697.34 | 99461.94 |
| | y | 71555.61 | 71682.09 | 71661.25 | 71461.61 |
| | z | 1174.918 | 1199.947 | 1174.827 | 1214.587 |
| **Module Weight** | (lb) | 313926 | 215561 | 318777 | 338379 |
| **Pick angle** | Swing | -82.3879 | 240.69 | -135 | 141.7098 |
| | Luffing | 71.74007 | 76.24902 | 70.47193 | 69.38369 |
| | Hoisting | 259.8923 | 265.858 | 257.9214 | 256.1288 |
| **Set angle (Calculation)** | Swing | -139.274 | 179.09 | -41.6327 | 203.5529 |
| | Luffing | 67.2481 | 61.46572 | 80.94699 | 69.55474 |
| | Hoisting | 252.4241 | 215.3887 | 270.487 | 216.83 |

* Tracking ID indicates the crane location in the database.

* All coordinates are based on the center point of the object.

# APPENDIX C: Object Information

| MODULE | | | 21 | Sequence | | 32 | |
|---|---|---|---|---|---|---|---|
| Module ID | Sequence | x | y | z | width | length | height |
| 22 | 31 | 99952 | 71516 | 1163 | 22 | 81 | 24 |
| 78 | 30 | 99976 | 71470 | 1163 | 22 | 53 | 24 |
| 117 | 25 | 99984 | 71742 | 1164 | 10 | 11 | 31 |

| MODULE | | | 32 | Sequence | | 19 | |
|---|---|---|---|---|---|---|---|
| Module ID | Sequence | x | y | z | width | length | height |
| 30 | 18 | 99797 | 71648 | 1162 | 64 | 20 | 22 |
| 31 | 17 | 99797 | 71672 | 1162 | 64 | 20 | 24 |
| 156 | 16 | 99782 | 71743 | 1183 | 23 | 20 | 19 |

| MODULE | | | 56 | Sequence | | 45 | |
|---|---|---|---|---|---|---|---|
| Module ID | Sequence | x | y | z | width | length | height |
| 11 | 40 | 99688 | 71539 | 1163 | 62 | 20 | 24 |
| 12 | 43 | 99626 | 71539 | 1187 | 120 | 24 | 23 |
| 29 | 21 | 99797 | 71590 | 1162 | 64 | 20 | 22 |
| 30 | 18 | 99797 | 71648 | 1162 | 64 | 20 | 22 |
| 31 | 17 | 99797 | 71672 | 1162 | 64 | 20 | 24 |
| 32 | 19 | 99797 | 71672 | 1188 | 54 | 20 | 25 |
| 72 | 41 | 99624 | 71539 | 1163 | 61 | 22 | 24 |
| 90 | 36 | 99757 | 71629 | 1163 | 20 | 98 | 23 |
| 91 | 37 | 99757 | 71639 | 1188 | 20 | 98 | 25 |
| 141 | 38 | 99757 | 71736 | 1164 | 20 | 38 | 23 |
| 142 | 39 | 99757 | 71736 | 1188 | 20 | 42 | 19 |
| 156 | 16 | 99782 | 71743 | 1183 | 23 | 20 | 19 |

| MODULE | | | 98 | Sequence | | 82 | |
|---|---|---|---|---|---|---|---|
| Module ID | Sequence | x | y | z | width | length | height |
| 11 | 40 | 99688 | 71539 | 1163 | 62 | 20 | 24 |
| 12 | 43 | 99626 | 71539 | 1187 | 120 | 24 | 23 |
| 13 | 28 | 99705 | 71515 | 1163 | 39 | 22 | 24 |
| 14 | 44 | 99626 | 71515 | 1187 | 118 | 22 | 21 |
| 17 | 11 | 99665 | 71509 | 1214 | 20 | 20 | 76 |

| 36 | 33 | 99679 | 71491 | 1164 | 67 | 24 | 18 |
|----|----|-------|-------|------|-----|----|----|
| 37 | 77 | 99626 | 71491 | 1180 | 120 | 24 | 24 |
| 38 | 78 | 99644 | 71491 | 1207 | 101 | 24 | 27 |
| 45 | 72 | 99554 | 71393 | 1163 | 58 | 24 | 22 |
| 46 | 73 | 99554 | 71393 | 1187 | 58 | 24 | 20 |
| 47 | 74 | 99645 | 71393 | 1163 | 61 | 24 | 22 |
| 48 | 75 | 99647 | 71393 | 1187 | 59 | 24 | 21 |
| 63 | 60 | 99491 | 71414 | 1187 | 20 | 36 | 22 |
| 64 | 59 | 99568 | 71414 | 1187 | 22 | 36 | 35 |
| 65 | 2 | 99669 | 71414 | 1187 | 22 | 37 | 22 |
| 72 | 41 | 99624 | 71539 | 1163 | 61 | 22 | 24 |
| 73 | 42 | 99626 | 71515 | 1163 | 75 | 22 | 23 |
| 79 | 76 | 99623 | 71491 | 1164 | 64 | 20 | 20 |
| 89 | 35 | 99689 | 71437 | 1163 | 57 | 12 | 23 |
| 92 | 68 | 99639 | 71452 | 1164 | 118 | 20 | 26 |
| 93 | 70 | 99639 | 71452 | 1188 | 118 | 20 | 24 |
| 94 | 69 | 99521 | 71452 | 1164 | 118 | 20 | 26 |
| 95 | 71 | 99521 | 71452 | 1188 | 118 | 20 | 25 |
| 96 | 80 | 99403 | 71452 | 1164 | 98 | 20 | 26 |
| 97 | 81 | 99403 | 71452 | 1188 | 118 | 20 | 21 |

# Appendix D: Result Example (Module 98: A* Algorithm)

- Raw result

| | Swing | Luffing | Hoisting | x | y | z | distance (ft) | Radius (ft) | Capacity (lb) | Safety factor (%) | speed (ft/min) | operation time (s) |
|---|---|---|---|---|---|---|---|---|---|---|---|---|
| 0 | 142 | 69 | 256 | -76 | 60 | 1 | 25.00 | 96.83 | 491600 | 79.97 | 47.90 | 31.32 |
| 1 | 142 | 69 | 231 | -76 | 60 | 26 | 9.98 | 96.83 | 491600 | 79.97 | 70.59 | 0.85 |
| 2 | 142 | 70 | 231 | -74.12 | 57.91 | 16.42 | 1.00 | 94.06 | 491600 | 79.97 | 47.90 | 1.25 |
| 3 | 142 | 70 | 230 | -74.12 | 57.91 | 17.42 | 1.00 | 94.06 | 491600 | 79.97 | 47.90 | 1.25 |
| 4 | 142 | 70 | 229 | -74.12 | 57.91 | 18.42 | 1.00 | 94.06 | 491600 | 79.97 | 47.90 | 1.25 |
| 5 | 142 | 70 | 228 | -74.12 | 57.91 | 19.42 | 1.00 | 94.06 | 491600 | 79.97 | 47.90 | 1.25 |
| 6 | 142 | 70 | 227 | -74.12 | 57.91 | 20.42 | 1.00 | 94.06 | 491600 | 79.97 | 47.90 | 1.25 |
| 7 | 142 | 70 | 226 | -74.12 | 57.91 | 21.42 | 1.00 | 94.06 | 491600 | 79.97 | 47.90 | 1.25 |
| 8 | 142 | 70 | 225 | -74.12 | 57.91 | 22.42 | 1.00 | 94.06 | 491600 | 79.97 | 47.90 | 1.25 |
| 9 | 142 | 70 | 224 | -74.12 | 57.91 | 23.42 | 1.00 | 94.06 | 491600 | 79.97 | 47.90 | 1.25 |
| 10 | 142 | 70 | 223 | -74.12 | 57.91 | 24.42 | 1.00 | 94.06 | 491600 | 79.97 | 47.90 | 1.25 |
| 11 | 142 | 70 | 222 | -74.12 | 57.91 | 25.42 | 1.00 | 94.06 | 491600 | 79.97 | 47.90 | 1.25 |
| 12 | 142 | 70 | 221 | -74.12 | 57.91 | 26.42 | 1.00 | 94.06 | 491600 | 79.97 | 47.90 | 1.25 |
| 13 | 142 | 70 | 220 | -74.12 | 57.91 | 27.42 | 1.00 | 94.06 | 491600 | 79.97 | 47.90 | 1.25 |
| 14 | 142 | 70 | 219 | -74.12 | 57.91 | 28.42 | 1.00 | 94.06 | 491600 | 79.97 | 47.90 | 1.25 |
| 15 | 142 | 70 | 218 | -74.12 | 57.91 | 29.42 | 1.00 | 94.06 | 491600 | 79.97 | 47.90 | 1.25 |
| 16 | 142 | 70 | 217 | -74.12 | 57.91 | 30.42 | 1.00 | 94.06 | 491600 | 79.97 | 47.90 | 1.25 |
| 17 | 142 | 70 | 216 | -74.12 | 57.91 | 31.42 | 1.00 | 94.06 | 491600 | 79.97 | 47.90 | 1.25 |
| 18 | 142 | 70 | 215 | -74.12 | 57.91 | 32.42 | 1.00 | 94.06 | 491600 | 79.97 | 47.90 | 1.25 |
| 19 | 142 | 70 | 214 | -74.12 | 57.91 | 33.42 | 1.00 | 94.06 | 491600 | 79.97 | 47.90 | 1.25 |
| 20 | 142 | 70 | 213 | -74.12 | 57.91 | 34.42 | 1.00 | 94.06 | 491600 | 79.97 | 47.90 | 1.25 |
| 21 | 142 | 70 | 212 | -74.12 | 57.91 | 35.42 | 1.00 | 94.06 | 491600 | 79.97 | 47.90 | 1.25 |
| 22 | 142 | 70 | 211 | -74.12 | 57.91 | 36.42 | 1.00 | 94.06 | 491600 | 79.97 | 47.90 | 1.25 |
| 23 | 142 | 70 | 210 | -74.12 | 57.91 | 37.42 | 1.00 | 94.06 | 491600 | 79.97 | 47.90 | 1.25 |
| 24 | 142 | 70 | 209 | -74.12 | 57.91 | 38.42 | 1.00 | 94.06 | 491600 | 79.97 | 47.90 | 1.25 |
| 25 | 142 | 70 | 208 | -74.12 | 57.91 | 39.42 | 1.00 | 94.06 | 491600 | 79.97 | 47.90 | 1.25 |
| 26 | 142 | 70 | 207 | -74.12 | 57.91 | 40.42 | 1.00 | 94.06 | 491600 | 79.97 | 47.90 | 1.25 |
| 27 | 142 | 70 | 206 | -74.12 | 57.91 | 41.42 | 1.00 | 94.06 | 491600 | 79.97 | 47.90 | 1.25 |
| 28 | 142 | 70 | 205 | -74.12 | 57.91 | 42.42 | 1.00 | 94.06 | 491600 | 79.97 | 47.90 | 1.25 |
| 29 | 142 | 70 | 204 | -74.12 | 57.91 | 43.42 | 1.00 | 94.06 | 491600 | 79.97 | 47.90 | 1.25 |
| 30 | 142 | 70 | 203 | -74.12 | 57.91 | 44.42 | 1.00 | 94.06 | 491600 | 79.97 | 47.90 | 1.25 |
| 31 | 142 | 70 | 202 | -74.12 | 57.91 | 45.42 | 1.00 | 94.06 | 491600 | 79.97 | 47.90 | 1.25 |
| 32 | 142 | 70 | 201 | -74.12 | 57.91 | 46.42 | 1.00 | 94.06 | 491600 | 79.97 | 47.90 | 1.25 |
| 33 | 142 | 70 | 200 | -74.12 | 57.91 | 47.42 | 1.00 | 94.06 | 491600 | 79.97 | 47.90 | 1.25 |
| 34 | 142 | 70 | 199 | -74.12 | 57.91 | 48.42 | 1.00 | 94.06 | 491600 | 79.97 | 47.90 | 1.25 |

| | | | | | | | | | | | | |
|---|---|---|---|---|---|---|---|---|---|---|---|---|
| 35 | 142 | 70 | 198 | -74.12 | 57.91 | 49.42 | 1.00 | 94.06 | 491600 | 79.97 | 47.90 | 1.25 |
| 36 | 142 | 70 | 197 | -74.12 | 57.91 | 50.42 | 1.00 | 94.06 | 491600 | 79.97 | 47.90 | 1.25 |
| 37 | 142 | 70 | 196 | -74.12 | 57.91 | 51.42 | 1.00 | 94.06 | 491600 | 79.97 | 47.90 | 1.25 |
| 38 | 142 | 70 | 195 | -74.12 | 57.91 | 52.42 | 1.00 | 94.06 | 491600 | 79.97 | 47.90 | 1.25 |
| 39 | 142 | 70 | 194 | -74.12 | 57.91 | 53.42 | 1.00 | 94.06 | 491600 | 79.97 | 47.90 | 1.25 |
| 40 | 142 | 70 | 193 | -74.12 | 57.91 | 54.42 | 1.00 | 94.06 | 491600 | 79.97 | 47.90 | 1.25 |
| 41 | 142 | 70 | 192 | -74.12 | 57.91 | 55.42 | 1.00 | 94.06 | 491600 | 79.97 | 47.90 | 1.25 |
| 42 | 142 | 70 | 191 | -74.12 | 57.91 | 56.42 | 1.00 | 94.06 | 491600 | 79.97 | 47.90 | 1.25 |
| 43 | 142 | 70 | 190 | -74.12 | 57.91 | 57.42 | 1.00 | 94.06 | 491600 | 79.97 | 47.90 | 1.25 |
| 44 | 142 | 70 | 189 | -74.12 | 57.91 | 58.42 | 1.00 | 94.06 | 491600 | 79.97 | 47.90 | 1.25 |
| 45 | 142 | 70 | 188 | -74.12 | 57.91 | 59.42 | 1.00 | 94.06 | 491600 | 79.97 | 47.90 | 1.25 |
| 46 | 142 | 70 | 187 | -74.12 | 57.91 | 60.42 | 1.00 | 94.06 | 491600 | 79.97 | 47.90 | 1.25 |
| 47 | 142 | 70 | 186 | -74.12 | 57.91 | 61.42 | 1.00 | 94.06 | 491600 | 79.97 | 47.90 | 1.25 |
| 48 | 142 | 70 | 185 | -74.12 | 57.91 | 62.42 | 1.00 | 94.06 | 491600 | 79.97 | 47.90 | 1.25 |
| 49 | 142 | 70 | 184 | -74.12 | 57.91 | 63.42 | 1.00 | 94.06 | 491600 | 79.97 | 47.90 | 1.25 |
| 50 | 142 | 70 | 183 | -74.12 | 57.91 | 64.42 | 1.65 | 94.06 | 491600 | 79.97 | 70.59 | 0.85 |
| 51 | 143 | 70 | 183 | -75.12 | 56.6 | 64.42 | 1.64 | 94.06 | 491600 | 79.97 | 70.59 | 0.85 |
| 52 | 144 | 70 | 183 | -76.09 | 55.28 | 64.42 | 1.64 | 94.05 | 491600 | 79.97 | 70.59 | 0.85 |
| 53 | 145 | 70 | 183 | -77.05 | 53.95 | 64.42 | 1.64 | 94.06 | 491600 | 79.97 | 70.59 | 0.85 |
| 54 | 146 | 70 | 183 | -77.98 | 52.6 | 64.42 | 1.64 | 94.06 | 491600 | 79.97 | 70.59 | 0.85 |
| 55 | 147 | 70 | 183 | -78.88 | 51.23 | 64.42 | 1.65 | 94.06 | 491600 | 79.97 | 70.59 | 0.85 |
| 56 | 148 | 70 | 183 | -79.76 | 49.84 | 64.42 | 1.64 | 94.05 | 491600 | 79.97 | 70.59 | 0.85 |
| 57 | 149 | 70 | 183 | -80.62 | 48.44 | 64.42 | 1.64 | 94.05 | 491600 | 79.97 | 70.59 | 0.85 |
| 58 | 150 | 70 | 183 | -81.45 | 47.03 | 64.42 | 1.64 | 94.05 | 491600 | 79.97 | 70.59 | 0.85 |
| 59 | 151 | 70 | 183 | -82.26 | 45.6 | 64.42 | 1.64 | 94.05 | 491600 | 79.97 | 70.59 | 0.85 |
| 60 | 152 | 70 | 183 | -83.05 | 44.16 | 64.42 | 1.64 | 94.06 | 491600 | 79.97 | 70.59 | 0.85 |
| 61 | 153 | 70 | 183 | -83.8 | 42.7 | 64.42 | 1.65 | 94.05 | 491600 | 79.97 | 70.59 | 0.85 |
| 62 | 154 | 70 | 183 | -84.54 | 41.23 | 64.42 | 1.64 | 94.06 | 491600 | 79.97 | 70.59 | 0.85 |
| 63 | 155 | 70 | 183 | -85.24 | 39.75 | 64.42 | 1.64 | 94.05 | 491600 | 79.97 | 70.59 | 0.85 |
| 64 | 156 | 70 | 183 | -85.92 | 38.26 | 64.42 | 1.65 | 94.05 | 491600 | 79.97 | 70.59 | 0.85 |
| 65 | 157 | 70 | 183 | -86.58 | 36.75 | 64.42 | 1.65 | 94.06 | 491600 | 79.97 | 70.59 | 0.85 |
| 66 | 158 | 70 | 183 | -87.21 | 35.23 | 64.42 | 1.63 | 94.06 | 491600 | 79.97 | 70.59 | 0.85 |
| 67 | 159 | 70 | 183 | -87.81 | 33.71 | 64.42 | 1.64 | 94.06 | 491600 | 79.97 | 70.59 | 0.85 |
| 68 | 160 | 70 | 183 | -88.38 | 32.17 | 64.42 | 1.64 | 94.05 | 491600 | 79.97 | 70.59 | 0.85 |
| 69 | 161 | 70 | 183 | -88.93 | 30.62 | 64.42 | 1.64 | 94.05 | 491600 | 79.97 | 70.59 | 0.85 |
| 70 | 162 | 70 | 183 | -89.45 | 29.06 | 64.42 | 1.64 | 94.05 | 491600 | 79.97 | 70.59 | 0.85 |
| 71 | 163 | 70 | 183 | -89.95 | 27.5 | 64.42 | 1.64 | 94.06 | 491600 | 79.97 | 70.59 | 0.85 |
| 72 | 164 | 70 | 183 | -90.41 | 25.93 | 64.42 | 1.65 | 94.05 | 491600 | 79.97 | 70.59 | 0.85 |
| 73 | 165 | 70 | 183 | -90.85 | 24.34 | 64.42 | 1.64 | 94.05 | 491600 | 79.97 | 70.59 | 0.85 |
| 74 | 166 | 70 | 183 | -91.26 | 22.75 | 64.42 | 1.63 | 94.05 | 491600 | 79.97 | 70.59 | 0.85 |
| 75 | 167 | 70 | 183 | -91.64 | 21.16 | 64.42 | 1.64 | 94.05 | 491600 | 79.97 | 70.59 | 0.85 |

| | | | | | | | | | | | |
|---|---|---|---|---|---|---|---|---|---|---|---|
| **76** | 168 | 70 | 183 | -92 | 19.56 | 64.42 | 1.64 | 94.06 | 491600 | 79.97 | 70.59 | 0.85 |
| **77** | 169 | 70 | 183 | -92.33 | 17.95 | 64.42 | 1.65 | 94.06 | 491600 | 79.97 | 70.59 | 0.85 |
| **78** | 170 | 70 | 183 | -92.63 | 16.33 | 64.42 | 1.64 | 94.06 | 491600 | 79.97 | 70.59 | 0.85 |
| **79** | 171 | 70 | 183 | -92.9 | 14.71 | 64.42 | 1.64 | 94.06 | 491600 | 79.97 | 70.59 | 0.85 |
| **80** | 172 | 70 | 183 | -93.14 | 13.09 | 64.42 | 1.64 | 94.06 | 491600 | 79.97 | 70.59 | 0.85 |
| **81** | 173 | 70 | 183 | -93.35 | 11.46 | 64.42 | 1.64 | 94.05 | 491600 | 79.97 | 70.59 | 0.85 |
| **82** | 174 | 70 | 183 | -93.54 | 9.83 | 64.42 | 1.64 | 94.06 | 491600 | 79.97 | 70.59 | 0.85 |
| **83** | 175 | 70 | 183 | -93.7 | 8.2 | 64.42 | 1.65 | 94.06 | 491600 | 79.97 | 70.59 | 0.85 |
| **84** | 176 | 70 | 183 | -93.83 | 6.56 | 64.42 | 1.64 | 94.06 | 491600 | 79.97 | 70.59 | 0.85 |
| **85** | 177 | 70 | 183 | -93.93 | 4.92 | 64.42 | 1.64 | 94.06 | 491600 | 79.97 | 70.59 | 0.85 |
| **86** | 178 | 70 | 183 | -94 | 3.28 | 64.42 | 1.64 | 94.06 | 491600 | 79.97 | 70.59 | 0.85 |
| **87** | 179 | 70 | 183 | -94.04 | 1.64 | 64.42 | 1.64 | 94.05 | 491600 | 79.97 | 70.59 | 0.85 |
| **88** | 180 | 70 | 183 | -94.06 | 0 | 64.42 | 1.64 | 94.06 | 491600 | 79.97 | 70.59 | 0.85 |
| **89** | 181 | 70 | 183 | -94.04 | -1.64 | 64.42 | 1.64 | 94.05 | 491600 | 79.97 | 70.59 | 0.85 |
| **90** | 182 | 70 | 183 | -94 | -3.28 | 64.42 | 1.64 | 94.06 | 491600 | 79.97 | 70.59 | 0.85 |
| **91** | 183 | 70 | 183 | -93.93 | -4.92 | 64.42 | 1.64 | 94.06 | 491600 | 79.97 | 70.59 | 0.85 |
| **92** | 184 | 70 | 183 | -93.83 | -6.56 | 64.42 | 1.65 | 94.06 | 491600 | 79.97 | 70.59 | 0.85 |
| **93** | 185 | 70 | 183 | -93.7 | -8.2 | 64.42 | 1.64 | 94.06 | 491600 | 79.97 | 70.59 | 0.85 |
| **94** | 186 | 70 | 183 | -93.54 | -9.83 | 64.42 | 1.64 | 94.06 | 491600 | 79.97 | 70.59 | 0.85 |
| **95** | 187 | 70 | 183 | -93.35 | -11.46 | 64.42 | 1.64 | 94.05 | 491600 | 79.97 | 70.59 | 0.85 |
| **96** | 188 | 70 | 183 | -93.14 | -13.09 | 64.42 | 1.64 | 94.06 | 491600 | 79.97 | 70.59 | 0.85 |
| **97** | 189 | 70 | 183 | -92.9 | -14.71 | 64.42 | 1.64 | 94.06 | 491600 | 79.97 | 70.59 | 0.85 |
| **98** | 190 | 70 | 183 | -92.63 | -16.33 | 64.42 | 1.65 | 94.06 | 491600 | 79.97 | 70.59 | 0.85 |
| **99** | 191 | 70 | 183 | -92.33 | -17.95 | 64.42 | 1.64 | 94.06 | 491600 | 79.97 | 70.59 | 0.85 |
| **100** | 192 | 70 | 183 | -92 | -19.56 | 64.42 | 1.64 | 94.06 | 491600 | 79.97 | 70.59 | 0.85 |
| **101** | 193 | 70 | 183 | -91.64 | -21.16 | 64.42 | 1.63 | 94.05 | 491600 | 79.97 | 70.59 | 0.85 |
| **102** | 194 | 70 | 183 | -91.26 | -22.75 | 64.42 | 1.64 | 94.05 | 491600 | 79.97 | 70.59 | 0.85 |
| **103** | 195 | 70 | 183 | -90.85 | -24.34 | 64.42 | 1.65 | 94.05 | 491600 | 79.97 | 70.59 | 0.85 |
| **104** | 196 | 70 | 183 | -90.41 | -25.93 | 64.42 | 1.64 | 94.05 | 491600 | 79.97 | 70.59 | 0.85 |
| **105** | 197 | 70 | 183 | -89.95 | -27.5 | 64.42 | 1.64 | 94.06 | 491600 | 79.97 | 70.59 | 0.85 |
| **106** | 198 | 70 | 183 | -89.45 | -29.06 | 64.42 | 1.64 | 94.05 | 491600 | 79.97 | 70.59 | 0.85 |
| **107** | 199 | 70 | 183 | -88.93 | -30.62 | 64.42 | 1.64 | 94.05 | 491600 | 79.97 | 70.59 | 0.85 |
| **108** | 200 | 70 | 183 | -88.38 | -32.17 | 64.42 | 1.64 | 94.05 | 491600 | 79.97 | 70.59 | 0.85 |
| **109** | 201 | 70 | 183 | -87.81 | -33.71 | 64.42 | 1.63 | 94.06 | 491600 | 79.97 | 70.59 | 0.85 |
| **110** | 202 | 70 | 183 | -87.21 | -35.23 | 64.42 | 1.65 | 94.06 | 491600 | 79.97 | 70.59 | 0.85 |
| **111** | 203 | 70 | 183 | -86.58 | -36.75 | 64.42 | 25.00 | 94.06 | 491600 | 79.97 | 47.90 | 31.32 |
| **112** | 203 | 70 | 208 | -86.58 | -36.75 | 39.42 | 0.00 | 94.06 | 491600 | 79.97 | 0.00 | 0.00 |

- Aggregated result

| | Movement | Start (degree) | End (degree) | Difference (degree) | Time Penalty (min) | Distance (ft) | Operation Time (s) |
|---|---|---|---|---|---|---|---|
| 0 | Hoisting | 256 | 231 | 25 | 0.75 | 25 | 31.3156715 |
| 1 | Luffing | 69 | 70 | 1 | 1 | 9.983932091 | 0.849996798 |
| 2 | Hoisting | 231 | 183 | 48 | 1 | 48 | 60.12608928 |
| 3 | Swing | 142 | 203 | 61 | 0.75 | 100.1354785 | 51.84980467 |
| 4 | Hoisting | 183 | 208 | 25 | 0 | 25 | 31.3156715 |

| | Module id | Computation Time (s) | Module Distance (ft) | Number of Movement | Number of Swing | Number of Luffing | Number of Hoisting | Total Operation time (min) |
|---|---|---|---|---|---|---|---|---|
| 0 | 98 | 25146.19857 | 208.1194106 | 5 | 1 | 1 | 3 | 6.424287229 |